

Review

Recent Applications and Strategies to Enhance Performance of Electrochemical Reduction of CO₂ Gas into Value-Added Chemicals Catalyzed by Whole-Cell Biocatalysts

Tuan Quang Anh Le

Faculty of Biotechnology, Ho Chi Minh City Open University, 35-37 Ho Hao Hon, District 1, Ho Chi Minh City 70000, Vietnam; tuan.lqa@ou.edu.vn; Tel.: +84-934-837989

Abstract: Carbon dioxide (CO₂) is one of the major greenhouse gases that has been shown to cause global warming. Decreasing CO₂ emissions plays an important role to minimize the impact of climate change. The utilization of CO₂ gas as a cheap and sustainable source to produce higher value-added chemicals such as formic acid, methanol, methane, and acetic acid has been attracting much attention. The electrochemical reduction of CO₂ catalyzed by whole-cell biocatalysts is a promising process for the production of value-added chemicals because it does not require costly enzyme purification steps and the supply of exogenous cofactors such as NADH. This study covered the recent applications of the diversity of microorganisms (pure cultures such as *Shewanella oneidensis* MR1, *Sporomusa* species, and *Clostridium* species and mixed cultures) as whole-cell biocatalysts to produce a wide range of value-added chemicals including methane, carboxylates (e.g., formate, acetate, butyrate, caproate), alcohols (e.g., ethanol, butanol), and bioplastics (e.g., Polyhydroxy butyrate). Remarkably, this study provided insights into the molecular levels of the proteins/enzymes (e.g., formate hydrogenases for CO₂ reduction into formate and electron-transporting proteins such as c-type cytochromes) of microorganisms which are involved in the electrochemical reduction of CO₂ into value-added chemicals for the suitable application of the microorganism in the chemical reduction of CO₂ and enhancing the catalytic efficiency of the microorganisms toward the reaction. Moreover, this study provided some strategies to enhance the performance of the reduction of CO₂ to produce value-added chemicals catalyzed by whole-cell biocatalysts.

Keywords: electrochemical reduction of CO₂; whole-cell biocatalysts; value-added chemicals; in silico study



Citation: Le, T.Q.A. Recent Applications and Strategies to Enhance Performance of Electrochemical Reduction of CO₂ Gas into Value-Added Chemicals Catalyzed by Whole-Cell Biocatalysts. *Processes* **2023**, *11*, 766. <https://doi.org/10.3390/pr11030766>

Academic Editor:
Gopalakrishnan Kumar

Received: 5 January 2023
Revised: 22 February 2023
Accepted: 24 February 2023
Published: 4 March 2023



Copyright: © 2023 by the author. Licensee MDPI, Basel, Switzerland. This article is an open access article distributed under the terms and conditions of the Creative Commons Attribution (CC BY) license (<https://creativecommons.org/licenses/by/4.0/>).

1. Introduction

Carbon dioxide (CO₂) is one of the major greenhouse gases that has been shown to cause global warming [1–3]. Decreasing CO₂ emissions plays an important role to minimize its impact on climate change. Several studies have been conducted to reduce CO₂ emissions including CO₂ capture and storage (CCS), CO₂ capture and utilization (CCU) [4–6], as well as utilizing an alternative renewable and sustainable energy source such as hydrogen (H₂) to replace fossil fuels [7–9]. The utilization of CO₂ gas as a cheap and sustainable source to produce higher value-added chemicals such as formic acid, butyrate, methanol, ethanol, polyhydroalkanoates, and polyurethane has been attracting much attention from many researchers [10–16]. It has been reported that CO₂ is biologically converted into value-added chemicals in various ways: (1) the hydration of CO₂ gas catalyzed by whole-cell formate hydrogen lyase to produce formic acid [17,18]; (2) the whole-cell photocatalytic production of value-added chemicals such as formate, succinate by microorganisms (e.g., *Shewanella oneidensis* MR1) [19]; or (3) the direct reduction of CO₂ catalyzed by isolated enzymes using NADH/NADPH as an electron donor to produce various organic chemicals [20,21]. For example, the enzymatic reduction of CO₂ catalyzed by formate dehydrogenase (from *Thiobacillus* sp. KNK65MA [22], and *Rhodobacter capsulatus* [23]) to produce

formic acid, or using enzyme cascades including three hydrogenases (i.e., formate dehydrogenase from *Candida boidinii*, formaldehyde dehydrogenase from *Pseudomonas* species, and alcohol dehydrogenase from *Saccharomyces cerevisiae*) [24,25] to produce methanol; and (4): the electrochemical reduction of CO₂ catalyzed by biocatalysts (i.e., isolated enzymes or microorganisms as whole-cell biocatalysts) and electrode-generated electrons to produce various value-added chemicals such as formate [13,26–28], methane [29,30], methanol [31], and acetate [32,33]. For example, the enzymatic electrochemical reduction of CO₂ to produce formate in the cathode chamber catalyzed by formate dehydrogenase from *Candida boidinii* using cofactor NADH and neutral red as the electron mediator [27] or catalyzed by a heterodisulfide reductase supercomplex including a heterodisulfide reductase (HdrABC), a formate dehydrogenase (FdhAB), and a Ni-Fe- hydrogenase (VhuABDGU) from *Methanococcus maripaludis* in a mediator-less electrochemical system [28]. The electrochemical reduction of CO₂ catalyzed by free enzymes to produce formate, carbon monoxide, and methanol is well reviewed by Yuan et al., 2019 [34] and Chiranjeevi et al., 2019 [35].

The electrochemical reduction of CO₂ catalyzed by whole-cell biocatalysts is a promising process for the production of value-added chemicals because it does not require costly enzyme purification steps and the supply of exogenous cofactors such as NADH [34]. The electrochemical reduction of CO₂ to produce value-added chemicals catalyzed by whole-cell biocatalysts occurs in the cathode chamber of a bio-electrochemical system which usually consists of an anode, a cathode, and a membrane separating the two (Figure 1a,b) [13,36–39]. The electrochemical reduction of CO₂ catalyzed by whole-cell biocatalysts in the cathode involves extracellular electron transfer (EET) from an electrode/cathode to microbes [39,40]. The EET is classified into two types: direct EET (Figure 1a) and indirect EET (Figure 1b). In the direct EET system, the microorganisms and electrode contact and exchange electrons directly without mediator compounds (e.g., *S. ovata* catalyzed for the production of acetate in the cathode chamber in the electrochemical reduction of CO₂ using a graphite electrode at a potential of -0.4 V vs. SHE without an electron mediator [38,41]). On the other hand an electron mediator such as methyl viologen, neutral red is required in an indirect EET system (e.g., *M. extoquens* AM1 catalyzed for the production of formate in the cathode chamber in the electrochemical reduction of CO₂ using a copper electrode at a potential of -0.75 V vs. Ag/AgCl with methyl viologen as an electron mediator [26,41]). Electron transfer systems in the electrochemical reduction of CO₂ catalyzed by whole-cell biocatalysts are well reviewed by Igarashi et al., 2017 [41] and Karthikeyan et al., 2019 [39].

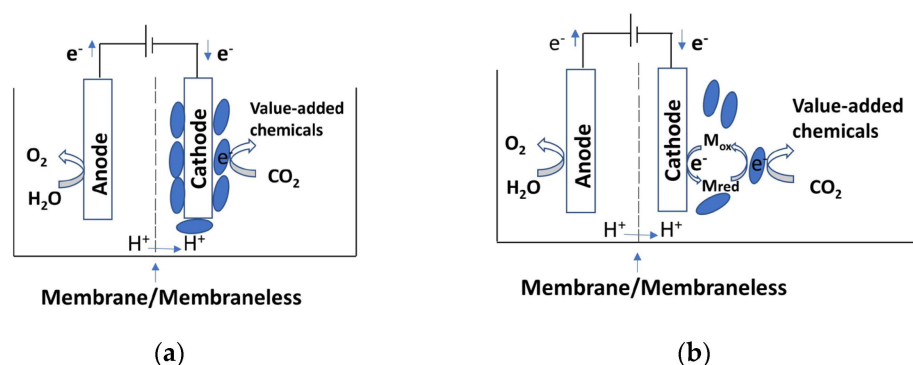


Figure 1. Schematic of two representative systems in electrochemical reduction of CO₂ to produce value-added chemicals catalyzed by whole-cell biocatalysts. (a) In direct EET [38]; (b) in indirect EET using electron mediator (Mox: oxidized form of mediator; Mred: reduced form of mediator) [13,26,39].

It was reported that various microorganisms (pure or enriched mixed cultures) have a capability as whole-cell biocatalysts for the electrochemical reduction of CO₂ to produce value-added chemicals such as formate, methane, acetate, butyrate [13,29,32,33,37,42–44]. Different microorganisms exhibited a diverse performance (production titer and production rate) for the electrochemical reduction of CO₂ to produce value-added chemicals.

For example, methane is produced from the electrochemical reduction of CO₂ catalyzed by *Methanobacterium palustre* [29,45] and acetate is mainly produced from the reduction of CO₂ by *Sporomusa ovata* [37]. Additionally, different strains of *Sporomusa* genera exhibited a different performance in the electrochemical CO₂ reduction to produce acetate (e.g., the acetate production by *Sporomusa ovata* DSM-2663 is ~2.6-fold higher than that by *Sporomusa ovata* DSM-3300) [32]. Understanding the catalytic characteristics of the microorganism as a whole-cell biocatalyst at the molecular level is essential not only for applying the microorganism in the electrochemical reduction of CO₂, but for enhancing the catalytic efficiency of the microorganism toward the reaction. It was reported that the performance of the reaction is also dependent on several other factors such as the reactor design and configuration [46], electrode design and materials [37,42,43], electron mediators [47], and poised cathode potential [48]. Recently, various studies have been performed to enhance the performance of the electrochemical reduction of CO₂ to produce value-added chemicals as well as to expand a range of products produced from the electrochemical reduction [37,42,43,48–51]. For example, the performance of the electrochemical reduction by *Sporomusa ovata* DSM 2662 to produce acetate using an reduced graphene oxide tetraethylene pentamine-modified carbon cloth (rCO-TEPA-CC) electrode is significantly higher than that using an untreated carbon cloth electrode (i.e., acetate production rates are $321 \pm 53 \text{ mM m}^{-2} \text{ day}^{-1}$ and $88 \pm 8 \text{ mM m}^{-2} \text{ day}^{-1}$ from the rGO-TEPA-CC electrode and untreated carbon cloth electrode, respectively) [42].

In this review, the recent application of microorganisms as whole-cell biocatalysts for the electrochemical reduction of CO₂ into various value-added chemicals will be discussed. Furthermore, some insights regarding the molecular levels of the microorganisms as a biocatalyst for the electrochemical reduction of CO₂ into value-added chemicals as well as strategies to increase the electrochemical reduction of CO₂ to produce value-added chemicals catalyzed by whole-cell biocatalysts will also be discussed.

2. Applications of Microorganisms as Whole-Cell Biocatalysts for Electrochemical Reduction of CO₂ into Value-Added Chemicals

2.1. Electrochemical Reduction of CO₂ to Produce Formate/Formic Acid by Whole-Cell Biocatalysts

Formate, which possesses good characteristics (e.g., non-flammable, non-toxic, and good electric energy generation compared to hydrogen, methanol, and ethanol), has been considered as a good energy storage molecule and a safe and renewable fuel [34,52,53]. It was reported that several microorganisms have been applied as whole-cell biocatalysts for the electrochemical reduction of CO₂ into formate/formic acid [13,26,49]. For example, several species of the *Methylobacteria* genus exhibited a good capacity as whole-cell biocatalysts for the electrochemical reduction of CO₂ into formate in the cathode chamber with a cathode potential of $-0.75 \text{ V vs. Ag/AgCl}$ using methyl viologen as the electron mediator. In this study, different *Methylobacterium* species showed a diverse performance as whole-cell biocatalysts on the electrochemical reduction of CO₂ to produce formate. The formate production by *Methylobacterium extorquens* AM1 was more than 2-fold compared to that by *Methylobacterium soli*, *Methylobacterium chloromethanicum*, *Methylobacterium platani*, *Methylobacterium suomiense*, and *Methylobacterium adhaesivum*. On the other hand, *Methylobacterium jeotgali* and *Methylobacterium dankookense* did not show capacity as biocatalysts for the reduction of CO₂ into formate [26]. The different results for the reduction of CO₂ into formate catalyzed from different *Methylobacterium* species in the same reaction conditions demonstrated the role of microorganisms as biocatalyst sources for the success of the reaction. Genome study on *Methylobacterium extorquens* AM1 revealed that the microorganism possesses multiple formate dehydrogenases [54] which could be the reason for the high capacity of the cell as a biocatalyst for the electrochemical reduction of CO₂ into formate. In addition to the role of whole-cell biocatalysts for the electrochemical reduction of CO₂ into formate, a study on the electrochemical reduction of CO₂ into formic acid catalyzed by formate dehydrogenase showed that the electron transfer from the electrode to the active center of the formate dehydrogenase is crucial for the final conversion [55]. The

electrochemical reduction of CO₂ into formate catalyzed by *Methylobacterium extorquens* AM1 in the presence of different concentrations of methyl viologen as the electron mediator revealed the role of electron transfer for the success of the CO₂ conversion (i.e., the electrochemical conversion of CO₂ into formate significantly increased with the increase in the concentration of methyl viologen as the electron mediator) [26]. The optimization of the reaction conditions (i.e., the concentration of microorganisms) was beneficial for the conversion of CO₂ into formate (i.e., a maximum 60 mM formate was produced after 80 h reaction catalyzed by *M. extorquens* AM1, as seen in Table 1 [26]). Additionally, *Methylobacterium extorquens* AM1 which grows and forms a biofilm on the carbon felt electrode showed the capability to catalyze for the electrochemical reduction of CO₂ to produce formate using neutral red as the electron mediator at a poised cathode potential of -0.75 V vs. Ag/AgCl [56]. Moreover, MeFDH1 recombinant *Methylobacterium extorquens* AM1 (F1A-P1 strain), an engineered *Methylobacterium extorquens* AM1 which lacks the *fdh1 α* gene and harbors recombinant plasmid pCM110(*fdh1*) for the recombinant expression of the *fdh1* gene, exhibited a better performance for the electrochemical reduction of CO₂ to produce formate. The performance of the electrochemical formate production from CO₂ by the MeFDH1 recombinant *Methylobacterium extorquens* AM1 grown in optimal conditions (supplemented with 2.0% *v/v* methanol and 60 μ M tungstate) is >3-fold better than that by *Methylobacterium extorquens* AM1 grown in the same conditions, as seen in Table 1 [49].

In addition to applying various *Methylobacterium* species as whole-cell biocatalysts for the electrochemical reduction of CO₂ into formate, *Shewanella oneidensis* MR-1 (*S. oneidensis* MR1), which is a facultative aerobic gram-negative bacterium and well known for its electron transfer system (i.e., including multiple cytochromes, reductases, iron-sulfur proteins, and quinones [57,58]) and possesses three formate dehydrogenases [59], was firstly applied as whole-cell biocatalysts for the electrochemical reduction of CO₂ into formic acid in our previous study [13]. *S. oneidensis* MR1, which was grown in various media and conditions based on the transcriptomic data of the microorganism, was applied as a whole-cell biocatalyst for the electrochemical reduction of CO₂ to produce formic acid in the cathode chamber with a poised cathode potential of -0.75 V vs. Ag/AgCl, with 10 mM methyl viologen as the electron mediator, and a copper electrode area of 3 cm². *S. oneidensis* MR-1, which was grown anaerobically in the optimized medium (Luria Bertani (LB) medium supplemented with 40 mM fumarate, 20 mM DL-lactate, and 1 mM nitrate) from our study, showed an improvement in catalytic capacity toward CO₂ conversion into formate compared to *M. extorquens* AM1 (i.e., 136.8 mM after 72 h reaction and 60 mM formate after 80 h reaction were produced from the electrochemical reactions of CO₂ catalyzed by *S. oneidensis* MR1 and *M. extorquens* AM1, respectively) [13,26]. The above-mentioned studies showed that microorganisms as whole-cell biocatalysts strongly impact on the performance of the formate production from CO₂. The optimization of the growth medium and conditions to obtain better versions of the microorganism (e.g., *Shewanella oneidensis* MR1) prior to applying the microorganism significantly increased the performance of the formate production from CO₂. Understanding the involvement of enzymes/proteins at a molecular level is beneficial for optimizing the growth conditions and medium for the microorganisms of interest as well as engineering the microorganism to obtain better versions of whole-cell biocatalysts from the original microorganism. Further discussion on the participating enzymes/proteins from microorganisms will be mentioned in section insights regarding the molecular basis of microorganisms as whole-cell biocatalysts.

2.2. Electrochemical Reduction of CO₂ to Produce Methane by Whole-Cell Biocatalysts

Methane is a potential greenhouse gas that causes climate change. However, methane, which has a high energy density and is a precursor to producing various organic molecules, has attracted attention from many researchers [45]. Various methanogenic microorganisms (i.e., pure, co-cultures, and mixed cultures) showed a capability as whole-cell biocatalysts for the electrochemical reduction of CO₂ to form methane [29,30,45,60,61]. It was reported that different methanogenic microorganisms showed a diverse performance as whole-cell

biocatalysts for the electrochemical reduction of CO₂ to produce methane [30,45]. For example, the performance of the electrochemical reduction of CO₂ into methane at a poised cathode potential of −0.7 V vs. SHE using a graphite rod electrode catalyzed by four methanogenic strains (i.e., *Methanococcus maripaludis* S2 DSM-14266, *Methanococcus vannielii* DSM-1224, *Methanoculleus submarinus* DSM-15122, and *Methanolacinia petrolearia* DSM-11571) is 53.6–62.8-fold higher than that catalyzed by *Methanobacterium congolense* DSM-7095 and *Methanosarcina mazei* Gö1 DSM-3647, respectively [45], as seen in Table 1. In this system, the methane production using a graphite rod electrode at a poised cathode potential of −0.7 V vs. SHE by pure strains (i.e., *Methanococcus maripaludis* S2 DSM-14266 and *Methanococcus vannielii* DSM-1224) reached a maximum value of 8.8 mmol m^{−2} d^{−1} methane) [45]. In the electrochemical reduction of CO₂ catalyzed by whole-cell biocatalysts to produce value-added chemicals, the electrode-generated electrons and electron transfer from the electrode to microbes are also important for the rate. Thus, lowering the poised potential at the cathode increased the methane from the electrochemical reduction of CO₂ (i.e., methane production rates from the electrochemical reduction of CO₂ by *Methanococcus maripaludis* MM901 at −0.6 V vs. SHE and −0.7 V vs. SHE are 0.05 and 0.125 μmol cm^{−2} h^{−1}, respectively (these values are based on 0.4 and 1 μmol h^{−1} methane produced from 150 mL catholyte using 8 cm² graphite rod electrode, respectively), as seen in Table 1) [30]. Additionally, co-cultures including *Methanococcus maripaludis* MM901 and the IS4 strain (DSM 15630) increased sharply the performance of the electrochemical reduction of CO₂ to produce methane compared to the only pure *Methanococcus maripaludis* MM901. The methane production from the co-culture at a poised potential of −0.5 V vs. SHE is 0.6–0.9 μmol cm^{−2} h^{−1}, which is about 12–18-fold higher than that by *Methanococcus maripaludis* MM901 (the methane production at a poised potential of −0.6 V vs. SHE is 0.05 μmol cm^{−2} h^{−1} based on 0.4 μmol h^{−1} from 8 cm² electrode surface area) [61], as seen in Table 1. The IS4 strain (DSM 15630) demonstrated its important role in the co-cultures for the methane production. It was reported that the IS4 strain (DSM 15630), a sulfate-reducing bacteria with the name of *Desulfoplia corrodens* [62], showed the capability to produce molecular hydrogen when grown on Fe(0) [61] and distribute electrons from cathodes to microorganisms that do not have the capability for electron uptake from electrodes to microorganisms [61].

Moreover, various studies applied enriched mixed cultures as whole-cell biocatalysts for the electrochemical reduction of CO₂ to produce methane [60,63,64], as seen in Table 1. For example, an enriched thermophilic mixed culture containing acetoclastic methanogens such as *Methanosaeta concilii* and *Desulfotomaculum peckii* showed a good performance as whole-cell biocatalysts for the electrochemical reduction of CO₂ to produce methane and acetate in a membrane-less single chamber with a cathode potential of −0.85 V vs. Ag/AgCl with a carbon disk electrode for the reaction at 60 °C. The acetate and methane production rate reached 9.43 g m^{−2} d^{−1} and 9.25 L m^{−2} d^{−1}, respectively [63]. The methane production (9.25 L m^{−2} d^{−1}) by the enriched thermophilic mixed culture at a poised cathode potential of −0.85 V vs. Ag/AgCl at 60 °C is significantly higher than the methane production of 70 mL m^{−2} d^{−1} (based on 17.5 μL of CH₄ produced, which detected a headspace volume after 4 h electrosynthesis using carbon felt (2.5 cm × 6 cm × 0.6 cm)) by enriched methanogenic microorganisms from a wastewater treatment plant in Asten [60]. *Desulfotomaculum peckii*, a sulfate-reducing bacteria which reduces a wide spectrum of electron acceptors [65], would be beneficial for the electron transfer from electrodes to the mixed culture for the improvement in the methane production from its methanogenic bacteria (e.g., *Methanosaeta concilii* in the mixed culture). Recently, Ni-based electrically conductive, catalytic, and porous hollow-fiber electrodes (CCPHF bundle) and a Ni-based porous hollow-fiber (Ni-PHF) increased the performance of the electrochemical reduction of CO₂ into methane at a poised cathode potential of −1.0 V vs. Ag/AgCl (i.e., the methane production from supplying CO₂ by passive diffusion through pores of the Ni-CCPHF cathode is 30-fold higher than that from supplying CO₂ in the reactor's headspace) [64], as seen in Table 1. The above-mentioned studies showed that the electrochemical reduction of CO₂ to

methane depended highly on the methanogenic microorganism as the whole cell biocatalyst, electron-generated cathode, and electron transfer from the cathode to the microorganism. Different methanogenic microorganisms exhibited a diverse performance as whole-cell biocatalysts for the electrochemical reduction of CO₂ to produce methane. The collaboration of a specialized electron-uptaking strain such as the IS4 strain with a methanogenic microorganism capable of producing methane (e.g., *Methanococcus maripaludis* MM901) is beneficial for the enhancement of the methane production from CO₂. Further discussion on the participating enzymes/proteins for methane production will be seen in the section insights regarding the molecular basis of microorganisms as biocatalysts.

2.3. Electrochemical Reduction of CO₂ to Produce Acetate and Other Multi-carbon Compounds

Acetate and other multi-carbon compounds, including carboxylate/carboxylic acid (e.g., butyrate, isobutyrate, caproate), alcohols (e.g., ethanol, butanol), and bioplastic polyhydroxybutyrate, exhibited a high value in various applications as a target for the electrochemical reduction of CO₂ [14,16,32,50,66]. Acetate, for example, is an important feedstock and precursor for the production of other products (e.g., vinyl acetate) [67]. Additionally, caproate/caproic acid is a feed additive, antimicrobial, and an important chemical platform for liquid fuels, lubricants, and bioplastics [68–71]. It was reported that the diversity of microorganisms demonstrates they are capable of being whole-cell biocatalysts for the production of a range of value-added chemicals, including carboxylates/carboxylic acids (e.g., acetate, butyrate, and caprolate), alcohols (e.g., ethanol, butanol), and bioplastics (e.g., polyhydroxybutyrate) from CO₂, as seen in Table 1 [16,32,38,48,50]. For example, several species of *Sporomusa* (e.g., *Sporomusa ovata* DSM-2662, *Sporomusa ovata* DSM-2663, *Sporomusa ovata* DSM-3300, *Sporomusa acidovorans*, and *Sporomusa malonica*) catalyzed for the electrochemical reduction of CO₂ to produce up to $61.1 \pm 18.1 \text{ mmol m}^{-2} \text{ d}^{-1}$ acetate at a poised cathode potential of -0.69 V vs. SHE using a graphite stick electrode [32], as seen in Table 1. In this study, different *Sporomusa* species showed a diverse performance as whole-cell biocatalysts for acetate production from the electrochemical reduction of CO₂. The performance of the acetate production catalyzed by *Sporomusa ovata* DSM-2663 was approximately 1.8-, 1.4-, 1.4-, and 4.7-fold higher than that catalyzed by *Sporomusa ovata* DSM-2662, *Sporomusa acidovorans*, *Sporomusa malonica*, *Sporomusa ovata* DSM-3300, respectively, as seen in Table 1. On the other hand, *Sporomusa aerivorans* did not show a capability as a whole-cell biocatalyst for the acetate production from the electrochemical reduction of CO₂ [32]. Remarkably, two *Sporomusa ovata* strains (i.e., DSM-2662 and DSM-2663) showed a significant difference toward the electrochemical reduction of CO₂ (i.e., the acetate production by *Sporomusa ovata* DSM-2663 and *Sporomusa ovata* DSM-2662 are $61.1 \pm 18.1 \text{ mmol m}^{-2} \text{ d}^{-1}$, $34.3 \pm 0.7 \text{ mmol m}^{-2} \text{ d}^{-1}$, respectively) [32]. The different performance of the acetate production for the reduction of CO₂ into acetate catalyzed from different *Sporomusa* species in the same reaction conditions demonstrated the role of microorganisms as biocatalyst sources for the success of the reaction. In addition to applying a single strain, co-cultures showed a good performance for the electrochemical reduction of CO₂ into acetate. For example, the collaboration of the strain IS4 (DSM 15630) (sulfate-reducing bacteria [62] could accept electrons from electrode) and *Acetobacterium woodi* (*Acetobacterium woodie*, acetogenic bacteria, converts CO₂ into acetate via the Wood-Ljungdahl pathway [72],) in co-cultures catalyzed for the electrochemical reduction of CO₂ to form acetate. In this system, the performance of the acetate production by co-cultures of the *Acetobacterium woodi* and strain IS4 (DSM 15630) reached $0.57\text{--}0.74 \text{ } \mu\text{mol cm}^{-2} \text{ h}^{-1}$ at -0.5 V vs. SHE , respectively [61], which is much better compared to that by *Acetobacterium woodii* at a poised cathode potential of -0.4 V vs. SHE (acetate was not detected) [33].

In addition to *Sporomomusa* species, various *Clostridium* species (e.g., *Clostridium ljundahlii*, *Clostridium aceticum*, *Clostridium scatologens* ATCC 25775^T, and *Moorella thermoacetica*) are capable as whole-cell biocatalysts for the electrochemical reduction of CO₂ to produce acetate and various multi-carbon compounds such as 2-oxo-butyrate, butyrate, ethanol, and butanol [14,33,48]. Different *Clostridium* species exhibited a diverse performance for the

electrochemical reduction of CO₂ to produce acetate and other multi-carbon compounds. For example, the electrochemical reduction of CO₂ catalyzed by *Clostridium ljundahlii* produced acetate (80 μmol) and only trace amounts of 2-oxo butyrate at a poised cathode potential of −0.4 V vs. SHE. On the other hand, *Clostridium acetivum* catalyzed for the electrochemical reduction of CO₂ to produce lower amounts of acetate (45 μmol) and higher amounts of 2-oxo butyrate (25 μmol) compared to *Clostridium ljundahlii* [33]. Moreover, microorganisms catalyzed for the electrochemical reduction of CO₂ to produce bioplastics (e.g., polyhydroxybutyrate). For example, a photoautotroph *Rhodospseudomonas palustris* TIE-1, a gram-negative purple non-sulfur bacterium which can use energy from light and obtain carbon from CO₂ under lighted conditions [73] and is capable of accepting electrons from a poised electrode [74], was applied as a whole-cell biocatalyst for the electrochemical reduction of CO₂ to produce polyhydroxybutyrate (PHB) [50]. In this system, the electrochemical reduction of CO₂ into PHB at a poised potential of +0.1 V vs. SHE in using a magnetite nanoparticle anchored graphene oxide deposited in a carbon felt (CF/rGO-MNPs) electrode showed a much better performance compared to that using an unmodified carbon felt electrode (i.e., the PHB yield using CF/rGO-MNP electrode and CF electrode are 91.31 ± 0.9 mg L^{−1} and 23.43 ± 0.9 mg L^{−1}, respectively) [50].

In addition to pure microbial cultures, mixed cell cultures were also applied for the electrochemical reduction of CO₂ to produce acetate and other multi-carbon chemicals such as carboxylates (e.g., butyrate, caprolate) [44,63,75] and alcohols (e.g., ethanol and isobutanol) [76]. For example, several studies applied mixed cultures as whole-cell biocatalysts for the reduction of CO₂ to produce acetate. For example, a mixed culture from activated sludge in a local sewage treatment plant in Chengdu, which consists of four major microorganisms (*Advenella mimigardefordensis*, *Acetobacterium woodii*, *Arcobacter cibarius*, *Wolinella succinogenes*) in the presence of methanogenic inhibitor 2-bromoethanesulfonic acid, showed a capacity to produce acetate and not methane in the cathode chamber at a potential in the range of −0.9 V to −1.1 V vs. Ag/AgCl using a carbon felt electrode (1.88 mM acetate was produced after 5 days) [44]. The presence of 2-bromoethanesulfonic acid, a specific inhibitor of methylcoenzyme M reductase (a key enzyme of methanogenesis) [30], is beneficial for enhancing the selectivity to acetate over methane in the electrochemical reduction of CO₂ to produce acetate. Additionally, applying mixed microbial cultures from natural environments (stormwater pond sediments, University of Queensland) and engineered anaerobic systems (Luggage Point Wastewater Treatment Plant anaerobic digester, Brisbane, Australia) at a potential of −0.85 V vs. SHE in a flow through reactor (FTR) produced acetate (maximum acetate concentration of 17.5 g L^{−1} and production rate of 9.8 L^{−1} d^{−1}) and a significant amount of value-added chemicals, up to six carbon compounds: n-butyrate (maximum of 9.3 g L^{−1} and 5.7 g L^{−1} d^{−1}) and n-caproate (maximum of 3.1 g L^{−1} and 2.0 g L^{−1} d^{−1}) by controlling the CO₂ loading rate (173 L d^{−1}) and hydraulic retention time [75]. The above-mentioned studies showed that different microorganisms exhibited a diverse performance (e.g., production titer, production rate) as well as a selectivity for the production of value-added chemicals.

To enhance the performance of the electrochemical reduction of CO₂ to produce acetate and high-value multiple-carbon molecules, different methods have been applied in recent studies. For example, different poised cathode potentials (e.g., −0.6 V, −0.8 V, −1.05 V, and −1.2 V vs. Ag/AgCl electrode) were applied in the electrochemical reduction of CO₂ catalyzed by *Clostridium scatologenes* ATCC 25775T as whole-cell biocatalysts. In this system, the production of acetate, butyrate, and ethanol from the electrochemical reduction at a poised potential of −1.2 V vs. Ag/AgCl was significantly higher than that from the reduction at a poised potential of −0.6 V vs. Ag/AgCl (i.e., the production of acetate, butyrate, and ethanol from the system with a poised potential of −1.2 V vs. Ag/AgCl are 0.44 g L^{−1}, 0.085 g L^{−1}, and 0.015 g L^{−1} on day 28, respectively), as seen in Table 1 [48]. The study demonstrated the role of electrode-generated electrons and the capability of *C. scatologenes* ATCC 25775T to utilize electrode-generated electrons to produce value-added chemicals (e.g., acetate, butyrate, and ethanol). Additionally, recent studies have developed

a wide range of electrodes to enhance the performance of the electrochemical reduction of CO₂ to produce acetate from the electrochemical reduction of CO₂, including chitosan-coated carbon cloth [43], rGO-TEPA-CC [42], porous nickel hollow fiber cathodes coated with carbon nanotubes (Ni-PHF/CNTs) [37], magnetite nanoparticle anchored graphene oxide deposited in a carbon felt (CF/rGO-MNPs) electrode [50], copper foam coated with a reduced graphene oxide electrode (rGO-CuF electrode), a reduced graphene oxide foam electrode (rGO foam) [77], and a 3D-graphene-coated carbon felt electrode (3D-GO-CF electrode) [51]. Thus, the modification of electrode materials improved the performance of the electrochemical reduction of CO₂ to produce acetate and multi-carbon compounds catalyzed by microorganisms as whole-cell biocatalysts. For example, the acetate production from CO₂ catalyzed by *Sporomusa ovata* DSM-2662 at a poised cathode potential of -0.69 V vs. SHE using a 3D-graphene-coated carbon felt electrode (3D-GO-CF electrode) and rGO-TEPA-CC electrode is much better than a carbon cloth or graphite stick electrode, as seen in Table 1. The acetate production from the electrochemical reduction of CO₂ catalyzed by *Sporomusa ovata* DSM-2662 at a poised cathode potential of -0.69 V vs. Ag/AgCl using a 3D-G-CF electrode is ~ 6.8 -fold higher than that using a carbon felt electrode and reached 925.5 ± 29.4 mM m⁻² d⁻¹ [51]. Additionally, the acetate and butyrate production by *Clostridium ljundadlii* CLJU_{BAPP} (integrating the butyric acid production pathway (BAPP) of *Clostridium acetobutylicum* into the *Clostridium ljundadlii*) using a Ni-P₁₅-modified carbon felt electrode (Ni-P₁₅/CF electrode) at a poised cathode potential of -1.05 V vs. Ag/AgCl were ~ 1.7 - and ~ 2.1 -fold higher than those ones using an unmodified carbon felt, respectively (i.e., the acetate and butyrate production by *Clostridium ljundadlii* CLJU_{BAPP} using a Ni-P₁₅/CF electrode reached 1.18 ± 0.01 g L⁻¹ and 0.67 ± 0.01 g L⁻¹, respectively) [78], (see Table 1). Moreover, other electrode materials (e.g., chitosan-coated carbon cloth, rGO-TEPA-CC, Ni-based PHF/CNTs electrodes) improved the performance for the electrochemical reduction of CO₂ into acetate compared to simple carbon electrodes (e.g., carbon cloth and carbon felt) or graphite stick electrode materials (see Table 1). It was reported that the modified electrodes (e.g., 3D-G-CF electrode) significantly increased the cell density on the surface of the electrodes and the current density compared to the unmodified carbon felt or carbon cloth (e.g., the current density of 3D-G-CF with *Sporomusa ovata* DSM-2662 and carbon felt with *Sporomusa ovata* DSM-2662 are 2450 ± 160 and 400 ± 100 mA m⁻², respectively) [51]. The above-mentioned studies showed that different microorganisms exhibited a diverse performance as whole-cell biocatalysts for the electrochemical reduction of CO₂ to produce acetate and multi-carbon compounds such as butyrate, caproate, and bioplastic polyhydroxy butyrate. The *Sporomusa* species showed a high selectivity toward the production of acetate from CO₂ and autotroph *Rhodospseudomonas palustris* TE1 showed a high selectivity toward PHB production. On the other hand, the product selectivity of the electrochemical reduction of CO₂ by the *Clostridium* species is dependent on the *Clostridium* strain itself and the reaction conditions. Understanding the involvement of the enzymes/proteins of the microorganisms catalyzed for the CO₂ reduction at a molecular level is essential for applying suitable microorganisms as whole-cell biocatalysts, optimizing the growth medium and conditions to obtain a better version of the microorganism as a whole-cell biocatalyst, and engineering the microorganism.

Table 1. Applications of pure and mixed cultures as whole-cell biocatalysts for electrochemical reduction of CO₂ gas into value-added chemicals.

Whole-Cell Biocatalysts	Dominant Strains in Pure and Mixed Cultures	Products	Cathode Potential	Cathode Electrode and Reaction Conditions	Production Rate and Titer	References
<i>Methylobacterium extorquens</i> AM1	<i>Methylobacterium extorquens</i> AM1	Formate	−0.75 V vs. Ag/AgCl	Copper electrode (1.5 cm × 2 cm), 25 °C	Formate: 60 mM after 80 h	[26]
MeFDH1 recombinant <i>Methylobacterium extorquens</i> AM1 grown in optimal medium ^a	MeFDH1 recombinant <i>Methylobacterium extorquens</i> AM1	Formate	−0.75 V vs. Ag/AgCl	Copper electrode (1.5 cm × 2 cm), 25 °C	Formate: >30 mM after 24 h; 2.53 mM h ^{−1} g-wet-cell ^{−1}	[49]
<i>Methylobacterium extorquens</i> AM1 grown in optimal medium ^a	<i>Methylobacterium extorquens</i> AM1	Formate	−0.75 V vs. Ag/AgCl	Copper electrode (1.5 cm × 2 cm), 25 °C	Formate: 0.77 mM h ^{−1} g-wet-cell ^{−1}	[49]
<i>Shewanella oneidensis</i> MR1	<i>Shewanella oneidensis</i> MR1	Formate	−0.75 V vs. Ag/AgCl	Copper electrode (1.5 cm × 2 cm), 25 °C	Formate: 136.8 mM after 72 h; 3.8 mM formate h ^{−1} g-wet-cell ^{−1} .	[13]
<i>Methanococcus maripaludis</i> MM901	<i>Methanococcus maripaludis</i> MM901	Methane	−0.6 V to −0.7 V vs. SHE	Graphite rod (8 cm ²), 30 °C	Methane: 0.4 μmol h ^{−1} at −0.6 V vs. Ag/AgCl and 1 μmol h ^{−1} at −0.7 V vs. Ag/AgCl	[30]
<i>Methanococcus maripaludis</i> MM1284 mutant (Δ <i>fru</i> Δ <i>frc</i> Δ <i>hmd</i> Δ <i>ohu</i> Δ <i>ohc</i> Δ <i>ehb</i>)	<i>Methanococcus maripaludis</i> MM1284 mutant (Δ <i>fru</i> Δ <i>frc</i> Δ <i>hmd</i> Δ <i>ohu</i> Δ <i>ohc</i> Δ <i>ehb</i>)	Methane	−0.6 V vs. SHE	Graphite rod (8 cm ²), 30 °C	Methane: 0.04 μmol h ^{−1}	[30]
<i>Methanococcus maripaludis</i> MM901 and Strain IS4 (DSM 15630) co-cultures	<i>Methanococcus maripaludis</i> MM901 and Strain IS4 (DSM 15630) co-cultures	Methane	−0.4 V to −0.5 V vs. SHE	Graphite bar electrode (8 cm ²), 30 °C	Methane: 0.10–0.14 μmol cm ^{−2} h ^{−1} at −0.4 V vs. SHE and 0.6–0.9 μmol cm ^{−2} h ^{−1} at −0.5 V vs. SHE	[61]
<i>Methanococcus vannielii</i> DSM-1224	<i>Methanococcus vannielii</i> DSM-1224	Methane, H ₂	−0.7 V vs. SHE	Graphite rod electrode (6.75 cm ² working surface area) ^c , 37 °C	Methane: 8.8 mmol m ^{−2} d ^{−1}	[45]
<i>Methanococcus maripaludis</i> S2 DSM-14266	<i>Methanococcus maripaludis</i> S2 DSM-14266	Methane, H ₂	−0.7 V vs. SHE	Graphite rod electrode (6.75 cm ² working surface area) ^c , 37 °C	Methane: 8.8 mmol m ^{−2} d ^{−1}	[45]
<i>Methanosarcina mazei</i> G61 DSM-3647	<i>Methanosarcina mazei</i> G61 DSM-3647	Methane, H ₂	−0.7 V vs. SHE	Graphite rod electrode (6.75 cm ² working surface area) ^c , 37 °C	Methane: 0.14 mmol m ^{−2} d ^{−1}	[45]
<i>Methanobacterium congolense</i> DSM-7095	<i>Methanobacterium congolense</i> DSM-7095	Methane, H ₂	−0.7 V vs. SHE	Graphite rod (6.75 cm ² working surface area) ^c , 37 °C	Methane: 4.1 mmol m ^{−2} d ^{−1}	[45]
<i>Methanoculleus submarinus</i> DSM-15122	<i>Methanoculleus submarinus</i> DSM-15122	Methane, H ₂	−0.7 V vs. SHE	Graphite rod (6.75 cm ² working surface area) ^c , 37 °C	Methane: 7.9 mmol m ^{−2} d ^{−1}	[45]
<i>Methanolacinia petrolearia</i> DSM-11571	<i>Methanolacinia petrolearia</i> DSM-11571	Methane, H ₂	−0.7 V vs. SHE	Graphite rod (6.75 cm ² working surface area) ^c , 37 °C	Methane: 7.5 mmol m ^{−2} d ^{−1}	[45]
Methanogenic microorganisms from wastewater treatment plant Asten (Austria).	N.D.	Methane, H ₂	−0.7 V vs. Ag/AgCl	Carbon felt (2.5 cm × 6 cm × 0.6 cm), 30–35 °C	17.5 μL Methane and 930 μL of H ₂ after 4 h.	[60]
Anaerobic sludge (Manfouha Wastewater treatment Plant, Riyadh, KSA)	Hydrogenotrophic Methanogens (>99%) including <i>Methanobacteriales</i> (<i>Methanobacterium</i>).	Methane	−1.0 V vs. Ag/AgCl	Ni-CCPHF bundle electrode, 30 °C, 100% CO ₂ was supplied by passive diffusion through pores of the electrode	Methane: 161.0 mmol m ^{−2} d ^{−1} ; H ₂ : 150.5 mmol m ^{−2} d ^{−1}	[64]
Anaerobic sludge (Manfouha Wastewater treatment Plant, Riyadh, KSA)	Hydrogenotrophic Methanogens (>99%) including <i>Methanobacteriales</i> (<i>Methanobacterium</i>).	Methane	−1.0 V vs. Ag/AgCl	Ni-CCPHF bundle electrode, 30 °C, 100% CO ₂ sparged in the reactor's headspace	Methane: 5.9 mmol m ^{−2} d ^{−1} ; H ₂ : 90.9 mmol m ^{−2} d ^{−1}	[64]
Anaerobic sludge (anaerobic digester of local wastewater treatment)	Acetoclastic methanogens (<i>Methanosaeta concilii</i> , <i>Desulfotomaculum peckii</i> , <i>Methanothermobacter wolfeii</i>)	Acetate, methane.	−0.85 V vs. Ag/AgCl	Carbon disk (diameter 6 cm, thickness 1.3 cm), 60 °C	Acetate: 9.43 g m ^{−2} d ^{−1} and 10.5 g/L acetate after 137 days; Methane: 9.25 L m ^{−2} d ^{−1} and 10.3 L methane after 137 days.	[63]

Table 1. Cont.

Whole-Cell Biocatalysts	Dominant Strains in Pure and Mixed Cultures	Products	Cathode Potential	Cathode Electrode and Reaction Conditions	Production Rate and Titer	Reference
Activated sludge (sewage treatment plant, Chengdu)	<i>Advenella mimigardefordensis</i> , <i>Acetobacterium woodii</i> , <i>Arcobacter cibarius</i> , <i>Wolinella succinogenes</i>	Acetate, no methane	−0.9 V to −1.1 V vs. Ag/AgCl	Carbon felt (4.5 cm × 4.5 cm), in presence of 2-bromoethanesulfonic.	Acetate: 1.88 mM after 5 days and 0.38 mM d ^{−1} at −0.9 V vs. Ag/AgCl and 2.35 mM d ^{−1} at −1.1 V vs. Ag/AgCl	[44]
<i>Sporomusa ovata</i> DSM-2663	<i>Sporomusa ovata</i> DSM-2663	Acetate	−0.69 V vs. SHE	Graphite stick (36 cm ²), 25 °C	Acetate: 61.1 ± 18.1 mmol m ^{−2} d ^{−1}	[32]
<i>Sporomusa ovata</i> DSM-3300	<i>Sporomusa ovata</i> DSM-3300	Acetate	−0.69 V vs. SHE	Graphite stick (36 cm ²), 25 °C	Acetate: 12.9 ± 5.6 mmol m ^{−2} d ^{−1}	[32]
<i>Sporomusa acidovorans</i>	<i>Sporomusa acidovorans</i>	Acetate	−0.69 V vs. SHE	Graphite stick (36 cm ²), 25 °C	Acetate: 44.1 ± 14.2 mmol m ^{−2} d ^{−1}	[32]
<i>Sporomusa malonica</i>	<i>Sporomusa malonica</i>	Acetate	−0.69 V vs. SHE	Graphite stick (36 cm ²), 25 °C	Acetate: 45.4 ± 4.9 mmol m ^{−2} d ^{−1} ,	[32]
<i>Sporomusa aerivirans</i>	<i>Sporomusa aerivirans</i>	Acetate	−0.69 V vs. SHE	Graphite stick (36 cm ²), 25 °C	Not detected products	[32]
<i>Sporomusa ovata</i> DSM-2662	<i>Sporomusa ovata</i> DSM-2662	Acetate	−0.69 V vs. SHE	Graphite stick (36 cm ²), 25 °C	Acetate: 34.3 ± 07.0 mmol m ^{−2} d ^{−1}	[32]
<i>Sporomusa ovata</i> DSM-2662	<i>Sporomusa ovata</i> DSM-2662	Acetate	−0.6 V vs. Ag/AgCl	Chitosan-coated carbon cloth (47 cm ²), 25 °C	Acetate: 229 ± 56 mM m ^{−2} d ^{−1}	[43]
<i>Sporomusa ovata</i> DSM-2662	<i>Sporomusa ovata</i> DSM-2662	Acetate	−0.6 V vs. Ag/AgCl	Carbon cloth (47 cm ²), 25 °C	Acetate: 30 ± 7 mM m ^{−2} d ^{−1}	[43]
<i>Sporomusa ovata</i> DSM-2662	<i>Sporomusa ovata</i> DSM-2662	Acetate	−0.69 V vs. SHE	rGO-TEPA-CC electrode (28 cm ²), Room Temp.	Acetate: 321 ± 53 mM m ^{−2} d ^{−1}	[43]
<i>Sporomusa ovata</i> DSM-2662	<i>Sporomusa ovata</i> DSM-2662	Acetate	−0.69 V vs. SHE	Carbon cloth (28 cm ²), Room Temp.	Acetate: 88 ± 8 mM m ^{−2} d ^{−1}	[42]
<i>Sporomusa ovata</i> DSM-2662	<i>Sporomusa ovata</i> DSM-2662	Acetate	−0.6 V vs. Ag/AgCl	Ni-based PHF/CNTs electrode (14.5 cm ²), Room Temp.	Acetate: 247 ± 17 mM m ^{−2} d ^{−1}	[37]
<i>Sporomusa ovata</i> DSM-2662	<i>Sporomusa ovata</i> DSM-2662	Acetate	−0.6 V vs. Ag/AgCl	Ni-based PHF electrode (13.5 cm ²), Room Temp.	Acetate: 145 ± 4 mM m ^{−2} d ^{−1}	[37]
<i>Sporomusa ovata</i> DSM-2662	<i>Sporomusa ovata</i> DSM-2662	Acetate	−0.69 V vs. SHE	Carbon felt (22.5 cm ²), Room Temp.	Acetate: 136.5 ± 43.5 mM m ^{−2} d ^{−1}	[51]
<i>Sporomusa ovata</i> DSM-2662	<i>Sporomusa ovata</i> DSM-2662	Acetate	−0.69 V vs. SHE	3D-G-CF electrode (22.5 cm ²), Room Temp.	Acetate: 925.5 ± 29.4 mM m ^{−2} d ^{−1}	[51]
<i>Sporomusa ovata</i> DSM-2662	<i>Sporomusa ovata</i> DSM-2662	Acetate, H ₂	−0.99 V vs. SHE	CuF electrode (36 cm ²), 25 °C	79.6 ± 24.4 mmol m ^{−2} day ^{−1} acetate; 2500.9 ± 461.4 mmol m ^{−2} d ^{−1} H ₂	[77]
<i>Sporomusa ovata</i> DSM-2662	<i>Sporomusa ovata</i> DSM-2662	Acetate, H ₂	−0.99 V vs. SHE	rGO foam electrode (36 cm ²), 25 °C	222.4 ± 33.1 mmol m ^{−2} d ^{−1} acetate; 301.1 ± 77.8 mmol m ^{−2} d ^{−1} H ₂	[77]
<i>Sporomusa ovata</i> DSM-2662	<i>Sporomusa ovata</i> DSM-2662	Acetate, H ₂	−0.99 V vs. SHE	rGO-CuF electrode (36 cm ²), 25 °C	1697.6 ± 298.1 mmol m ^{−2} d ^{−1} acetate; 2599.2 ± 800.7 mmol m ^{−2} d ^{−1} H ₂	[77]
<i>Moorella thermoacetica</i>	<i>Moorella thermoacetica</i>	Acetate	−0.4 V vs. SHE	Graphite stick (65 cm ²)	Acetate: ~60 μmol after 6 days	[33]
<i>Acetobacterium woodii</i> and Strain IS4 (DSM 15630) co-cultures	<i>Acetobacterium woodii</i> and Strain IS4 (DSM 15630) co-cultures	Acetate	−0.4 V to −0.5 V vs. SHE	Graphite bar (8 cm ²), 30 °C	0.21–0.23 μmol cm ^{−2} h ^{−1} at −0.4 V vs. SHE; 0.57–0.74 μmol cm ^{−2} h ^{−1} at −0.5 V vs. SHE	[61]
<i>Clostridium ljundahlii</i>	<i>Clostridium ljundahlii</i>	Acetate, formate, 2-oxobutyrate	−0.4 V vs. SHE	Graphite stick (65 cm ²)	Acetate: ~80 μmol, formate (minor amount), 2-oxobutyrate (trace amount) after 6 days	[33]

Table 1. Cont.

Whole-Cell Biocatalysts	Dominant Strains in Pure and Mixed Cultures	Products	Cathode Potential	Cathode Electrode and Reaction Conditions	Production Rate and Titer	Reference
^b <i>Clostridium ljundahlia</i> CLJU _{BAPP}	<i>Clostridium ljundahlia</i> CLJU _{BAPP}	Acetate, butyrate	−1.05 V vs. Ag/AgCl	Carbon felt electrode (50 mm × 50 mm × 50 mm, length × width × thickness)	Acetate: 0.1 g L ^{−1} d ^{−1} , 0.68 ± 0.03 g L ^{−1} ; Butyrate: 0.1 g L ^{−1} d ^{−1} , 0.31 ± 0.02 g L ^{−1}	[78]
<i>Clostridium ljundahlia</i> CLJU _{BAPP}	<i>Clostridium ljundahlia</i> CLJU _{BAPP}	Acetate, Butyrate	−1.05 V vs. Ag/AgCl	Ni-P ₁₅ /CF electrode (50 mm × 50 mm × 50 mm, length × width × thickness)	Acetate: 0.17 g L ^{−1} d ^{−1} , 1.18 ± 0.01 g L ^{−1} ; Butyrate: 0.1 g L ^{−1} d ^{−1} , 0.67 ± 0.01 g L ^{−1}	[78]
<i>Clostridium acetium</i>	<i>Clostridium acetium</i>	Acetate, 2-oxobutyrate	−0.4 V vs. SHE	Graphite stick (65 cm ²)	~45 μmol acetate; ~25 μmol 2-oxobutyrate after 7 days	[33]
<i>Clostridium scatologens</i> ATCC 25775 ^T	<i>Clostridium scatologens</i> ATCC 25775 ^T	Acetate, butyrate, Ethanol	−0.6 V vs. Ag/AgCl	Carbon felt (50 mm × 50 mm × 50 mm), 25 ± 2 °C.	0.03 g/L acetic acid; 0.01 g/L butyric acid; 0.0 g/L ethanol after 28 days.	[48]
<i>Clostridium scatologens</i> ATCC 25775 ^T	<i>Clostridium scatologens</i> ATCC 25775 ^T	Acetate, Butyrate, Ethanol	−0.8 V vs. Ag/AgCl	Carbon felt (50 mm × 50 mm × 50 mm), 25 ± 2 °C.	0.095 g/L acetic acid; 0.051 g/L butyric acid; 0.01 g/L ethanol after 28 days.	[48]
<i>Clostridium scatologens</i> ATCC 25775 ^T	<i>Clostridium scatologens</i> ATCC 25775 ^T	Acetate, Butyrate, Ethanol	−1.05 V vs. Ag/AgCl	Carbon felt (50 mm × 50 mm × 50 mm), 25 ± 2 °C.	0.301 g/L acetic acid; 0.059 g/L butyric acid; 0.013 g/L ethanol after 28 days.	[48]
<i>Clostridium scatologens</i> ATCC 25775 ^T	<i>Clostridium scatologens</i> ATCC 25775 ^T	Acetate, Butyrate, Ethanol	−1.2 V vs. Ag/AgCl	Carbon felt (50 mm × 50 mm × 50 mm), 25 ± 2 °C.	0.44 g/L acetic acid; 0.085 g/L butyric acid; 0.015 g/L ethanol after 28 days.	[48]
Mixed cultures (sediment from a bog, Black Moshannon Park, Philipsburg, PA).	<i>Trichococcus palustris</i> 47–62%), <i>Oscillibacter</i> sp. (10–24%), <i>Clostridium</i> sp. (5–21%), <i>Desulfotomaculum</i> sp.; <i>Tissierella</i> sp.	Acetate; Propionate; Butyrate; Butanol; Ethanol	−0.4 V vs. SHE	Carbon fiber rods (14.7 cm ²)	Acetate: 1.90 ± 0.73 g L ^{−1} ; Propionate: 2.09 ± 0.56 g L ^{−1} ; butyrate: 2.25 ± 0.20 g L ^{−1} ; Butanol: 26.82 ± 0.00 mg L ^{−1} ; Ethanol: 16.04 mg L ^{−1}	[16]
Mixed cultures (stormwater pond sediments and Luggage Point Wastewater treatment Plant, Brisbane)	N.D.	Acetate, butyrate, caproate	−0.85 V vs. SHE	Carbon felt (25.5 cm ³), Flow through reactor (FTR)	Acetate: 17.5 g L ^{−1} , 9.8 L ^{−1} d ^{−1} ; n-butyrate: 9.3 g L ^{−1} , 5.7 g L ^{−1} d ^{−1} ; n-caproate: 3.1 g L ^{−1} , 2.0 g L ^{−1} d ^{−1}	[75]
<i>Rhodopseudomonas palustris</i> TIE-1	<i>Rhodopseudomonas palustris</i> TIE-1	Polyhydroxybutyrate (PHB)	+0.1 V vs. SHE	Carbon felt (1 × 1 cm ²), 25 °C	PHB: 23.43 ± 1.29 mg L ^{−1}	[50]
<i>Rhodopseudomonas palustris</i> TIE-1	<i>Rhodopseudomonas palustris</i> TIE-1	Polyhydroxybutyrate (PHB)	+0.1 V vs. SHE	CF/rGO-MNPs electrode (1 × 1 cm ²), 25 °C	PHB: 91.31 ± 0.9 mg L ^{−1}	[50]

SHE: Standard hydrogen electrode; Optimal medium. ^a: Medium supplemented with 2.0% *v/v* Methanol and 60 μM tungstate [49]; ^b: Ni-CCPHF bundle: Ni-CCPHF bundle (8 Ni-CCPHFs; 10 cm long each with outer diameter of 0.09 cm) electrode; Graphite rod (6.75 cm² working surface area); ^c: 1.4 cm diameter × 15 cm length, 4.5 cm submerged into the media; Room Temp.: Room temperature. N.D.: Not determined.

3. Insights regarding Molecular Basis of Microorganisms as Whole-Cell Biocatalysts for the Electrochemical Reduction of CO₂ to Produce Value-Added Chemicals

Understanding, at molecular levels, which proteins/enzymes from potential microorganisms are involved in the electrochemical reduction of CO₂ into value-added chemicals such as formate, methane, and acetate would be beneficial for the enhancement of the performance of the microorganisms as whole-cell biocatalysts for the electrochemical synthesis.

3.1. Understanding Reduction of CO₂ into Formate or Formic Acid Catalyzed by Whole-Cell Biocatalysts

It was reported that formate dehydrogenases (FDHs) catalyze for the interconversion of CO₂ into formate [23,55,79]. Formate dehydrogenase from *Rhodobacter capsulatus*, which belongs to metal and NAD⁺-dependent FDH, requires NADH cofactors for the CO₂ reduction into formate [23]. On the other hand, a tungsten-containing formate dehydrogenase from *Syntrophobacter fumaroxidans* catalyzes for the electrochemical reduction of CO₂ into formate and uses electrode-generated electrons and methyl viologen as the electron mediator [55]. Whole-genome analysis revealed the presence of formate dehydrogenases in *M. extorquens* AM1 and *S. oneidensis* and their role in the reduction of CO₂ to produce formate. *M. extorquens* AM1 possesses three formate dehydrogenases, a tungsten-containing NAD-linked FDH (FDH1) encoded by the *fdh1BA* gene and two additional FDHs, FDH2 which is encoded by one cluster (*fdh2CDAD*) and is a four subunit FDH and homologous to molybdenum FDH of *Ralstonia eutropha* and FDH3 which is encoded by the *fdhABC* gene and is a three subunit and homologous to FDH from *Wolinella succinogens* [80]. The mutant-based analysis of *M. extorquens* AM1 demonstrated that formate dehydrogenase 1, a tungsten-containing FDH encoded by two genes, *fdh1AB* [80] of *M. extorquens* AM1, plays a key role in the reduction of CO₂ to produce formate (i.e., *M. extorquens* AM1 mutant lacking the *fdh1alpha* or *fdh1beta* gene lost capacity for the electrochemical reduction of CO₂ into formate compared to its wild type) [49]. In addition, the *M. extorquens* AM1 mutant (a strain knocked-out *fdh1A* and harbored PCM110(*fdh1*) for the recombinant FDH1 of *M. extorquens* AM1) which was grown in optimal mediums and conditions for a greater expression level of the recombinant FDH1 showed a better catalytic performance toward the electrochemical reduction of CO₂ into formate compared to the wild type. Genome sequence analysis showed that *S. oneidensis* MR-1 possesses three *fdh* genes coding for formate dehydrogenases (FDHs) (i.e., *fdhGHI* [SO_0101 to SO_0103], *fdhA1B1C1* [SO_4508 to SO_4511], and *fdhA2B2C2* [SO_4512 to SO_4515]) and 39 c-type cytochromes [59]. *S. oneidensis* MR-1 consists of various electron-transporting proteins for the reduction of metal ions. The MtrCAB complex, encoded by *MtrCAB operon*, includes MtrC (outer-membrane decaheme-binding c-type cytochrome), MtrA (periplasmic c-type cytochrome), and MtrB (transmembrane c-type cytochrome bridging for MtrA and MtrC) and functions directly for the reduction of metal ions [81,82]. In addition, the MtrDEF complex which is encoded by the *MtrDEF* gene cluster (a paralog of *MtrCAB* genes and expressed under separate promoters from the *MtrCAB*) also plays a role in the reduction of metal ions [81]. Transcriptomes of *S. oneidensis* MR1 on the impact of the growth medium for the expression of the target proteins/enzymes showed that electron receptors, such as fumarate and nitrate, under anaerobic conditions are beneficial for the expression of formate dehydrogenases and various cytochromes [83]. The optimization of the growth medium and conditions of the *S. oneidensis* MR1, which aimed to increase the expression level of formate dehydrogenases and electron-transporting proteins based on the transcriptomic data of the bacteria, was performed in our group. As a result, we found that *S. oneidensis* MR1, which was anaerobically grown in an optimal medium (LB medium in the presence of fumarate, nitrate, and lactate), increased sharply compared to that catalyzed by the cell aerobically grown in the LB medium [13]. The study demonstrated the role of formate dehydrogenases and electron-transporting proteins such as MtrC, MtrB, and MtrA in *S. oneidensis* MR1 for the electrochemical reduction of CO₂ into formic acid [13]. The works presented here demonstrated the catalytic capability of the microorganisms (e.g., *M. extorquens* AM1 and *S. oneidensis* MR1) as whole-cell biocatalysts

for the electrochemical reduction of CO₂ at a molecular level. Optimizing the growth medium and conditions to increase the expression level of the critical proteins/enzymes (e.g., FDHs, MtrABC) in the microorganisms (e.g., *M. extorquens* AM1 and *S. oneidensis* MR1), thereby enhanced the performance of the electrochemical reduction of CO₂ catalyzed by the microorganisms which were grown in optimized mediums and conditions. This would be a good example for the further improvement in the catalytic efficiency of conventional microorganisms as whole-cell biocatalysts in the microbial electrochemical reduction of CO₂.

3.2. Understanding Reduction of CO₂ into Methane by Methanogenic Bacteria

In methanogenic bacteria, H₂ is used as the primary electron donor in the reduction of CO₂ into methane. The reduction of CO₂ into methane occurred in the following multiple steps: (1): CO₂ binds to methanofuran (MFR) and reduces to formyl-MFR (CHO-MFR) catalyzed by formylmethanofuran dehydrogenase. This step is coupled with reduced ferredoxin (Fd) via a membrane-bound energy conserving hydrogenase (Ech); (2): the formyl group of formyl-MFR is transferred to tetrahydromethanopterin (H₄MPT) to form formyl-H₄MPT (CHO-H₄MPT) catalyzed by formyl-MFR:H₄MPT transferase; (3) the formyl group of formyl-H₄MPT is then dehydrated to methenyl-H₄MPT (CH≡H₄MPT) catalyzed by N⁵, N¹⁰-methenyl-H₄MPT cyclohydrolase; (4) methenyl-H₄MPT is then sequentially reduced to methylene-H₄MPT (CH₂=H₄MPT) catalyzed by N⁵, N¹⁰-methylene-H₄MPT dehydrogenase (F420 dependent) and N⁵, N¹⁰-Methynene-H₄MPT dehydrogenase (hydrogen dependent); (5): methene-H₄MPT is reduced to methyl-H₄MPT (CH₃-H₄MPT) catalyzed by N⁵, N¹⁰-methylene-H₄MPT reductase; (6): the methyl group of H₄MPT is transferred to CoM to form methyl-Coenzyme M (CH₃-CoM) catalyzed by methyl-H₄MPT:HS-CoM methyltransferase (Mtr), which is a membrane-bound complex; and (7): methyl-CoM is finally reduced to methane (CH₄) using coenzyme B (CoB) as the electron donor by methyl coenzyme M reductase (Mcr, which is a key enzyme in methanogenesis) [84,85]. It is thought that methyl-coenzyme M reductase is a rate-limiting enzyme for methanogenesis in methanogenic archaea [86]. In the electrochemical reduction of CO₂ into methane by microorganisms as whole-cell biocatalysts, the electron transferring from electrodes to microorganisms is important. It was reported that several free and surface-associated redox enzymes, such as hydrogenases from methanogenic archaeon (e.g., *Methanococcus maripaludis*), play an important role in the mediating electron transfer from electrodes to methanogenic microbes. Thus, the hydrogenase deletion mutant (i.e., *Methanococcus maripaludis* MM1284 mutant) which carries deletions of six genes coding for hydrogenases (i.e., *fru*, *frc*, *hmd*, *vhu*, *vhc*, and *ehb*) only retained 10% of the catalytic capability of the *Methanococcus maripaludis* MM901 wild type for the electrochemical reduction of CO₂ to produce methane at a poised potential of −0.6 V vs. SHE (i.e., the methane production by *Methanococcus maripaludis* MM1284 mutant and *Methanococcus maripaludis* MM901 wild type are 0.04 μmol h^{−1} and 0.4 μmol h^{−1}, respectively). The study demonstrated the role of hydrogenases in *Methanogenic* microorganisms and hydrogen as an intermediate as well as hydrogen-independent electron uptake from the electrode [30]. Understanding the importance of proteins/enzymes at a molecular level in methanogenic bacteria as biocatalysts is beneficial to obtaining better whole-cell biocatalysts for the electrochemical reduction of CO₂ into methane.

3.3. Understanding Reduction of CO₂ into Acetate and Other Multi-carbon Compounds by the Whole-Cell Biocatalysts

It is thought that the anaerobic conversion of CO₂ and H₂ into acetate by acetogenic bacteria follows the reductive acetyl-CoA pathway [85,87]. The pathway includes multiple steps: (1) CO₂ reduction into formate catalyzed by formate dehydrogenases; (2) formate to formyl tetrahydrofolate (THF) catalyzed by formyl-THF synthetase; (3–4) formyl-THF is subsequently converted into methylene-THF catalyzed by methenyl-THF cyclohydrolase and methylene-THF dehydrogenase; (5) methylene-THF is converted into methyl-THF catalyzed by methylene-THF reductase; (6–7) methyl-THF is subsequently converted into

acetyl-CoA catalyzed by methyl-transferase and carbon monoxide dehydrogenase/acetyl-CoA synthase; and (8) acetyl-CoA is finally converted into acetate [88]. Genome analysis of the *Sporomusa* strain An4, which shares 99% of its average nucleotide identity with *Sporomusa ovata* strain H1, revealed the presence of all genes coding for the acetyl-CoA pathway (e.g., methenyl-THF cyclohydrolase, methylene-THF dehydrogenase, acetyl-CoA synthase, and formate dehydrogenase genes) [89]. The significant difference in the catalytic efficiency of various species of *Sporomusa* (i.e., *Sporomusa ovata* DSM-2662, *Sporomusa ovata* DSM-2663, *S. ovata* DSM-3300, *S. acidovorans*, *S. malonica*, *S. aerivorans*) as biocatalysts in the above-mentioned study for the electrochemical reduction of CO₂ into acetate demonstrated the role of key enzymes/proteins involved in the reduction of CO₂. Genome analysis between *S. ovata* DSM-2663 and *S. ovata* DSM-2662 showed that *S. ovata* DSM-2663 had 69 genome variations compared to that of *S. ovata* DSM-2662 such as a base substitution in a subunit of the NADP-reducing dehydrogenases (*hmdD2*) coupled with the oxidation of molecular H₂ and reduction of NADP into NADPH [32]. It is reported that *Sporomusa* species (i.e., *S. acidovorans* DSM 3132, *S. aerivorans* DSM 13326, *S. malonica* DSM 5090, *S. ovata* DSM 2662, *S. sphaeroides* strain E, *S. silvacetica* DSM 10669, *S. termitida*) consisting of c-type or b-type cytochromes and mena quinones in electron transporting systems [90] would be essential for electron transfer from electrodes to the *Sporomusa* species in the electrochemical reduction of CO₂ to form value-added chemicals. Additionally, the proteomic analysis of *Sporomusa* strain An4 revealed that the products of c-type cytochrome biosynthesis genes, *ccmA*, *ccmB*, and *ccmC*, had a high protein abundance in *Sporomusa* strain An4 when grown with nitrate [89]. Modifying the nitrate content in the growth medium of the *Sporomusa* species prior to applying the microorganisms as whole-cell biocatalysts would be beneficial for the performance of the electrochemical reduction. In addition to the genome analysis, the study of the impact of tungstate in the growth medium of *Sporomusa ovata* DSM-2662 showed that an increase in the tungstate concentration (in the range of 0.01 μM and 0.1 μM) on the growth medium (DZMZ311 medium) significantly increased the production of acetate in the microbial electrosynthesis from CO₂ and H₂ as reactants (i.e., acetate production is $141.2 \pm 56.6 \text{ mmol m}^{-2} \text{ day}^{-1}$ and $380.0 \pm 20.0 - 1694.5 \pm 678.6 \text{ μM m}^{-2} \text{ day}^{-1}$ in the DZMZ311 medium in the presence of 0.1 μM and 0.01 μM tungstate, respectively) [91]. It was reported that tungsten is a cofactor for the acetogenic formate dehydrogenase involved in the Wood–Ljungdahl (WL) pathway and the increase in the tungstate concentration in the DZMZ311 medium significantly increased in the transcript abundance of *fddA2* (SOV_3c08790) encoding for α-subunits of formate dehydrogenase 2 (FDH2) of *S. ovata* (i.e., 3.3 ± 0.2-fold [91]). The increase in the expression level of the involved enzymes of the WL pathway of the acetogenic bacteria (e.g., formate dehydrogenases) led to an increase in acetate production in the microbial electrosynthesis catalyzed by the acetogenic bacteria (e.g., *S. ovata* DSM-2662).

As mentioned above, *Clostridium* (e.g., *Clostridium ljundahlii*, *Clostridium aceticum*, *Clostridium scatologens* ATCC 25775^T) exhibited a capability to produce longer carbon compounds (e.g., butyrate and caproate). It is hypothesized that short-chain carboxylates (e.g., lactate, acetate) could be chain elongated to longer-chain carboxylates (e.g., caproate) via the reverse β-oxidation pathway [66,70,92]. The chain elongation by microorganisms is an anaerobic metabolism of microorganisms by a combination of carboxylates (e.g., acetate) with more reduced compounds (e.g., ethanol) to produce a long-chain carboxylate (e.g., butyrate, caproate) [93,94]. It reported that the *Clostridium* species (e.g., *Clostridium kluyveri*) is capable of converting acetate and ethanol to produce longer carboxylic acids (e.g., butrate, caproate, caprylate) by a chain elongation process [71].

4. Strategies to Enhance Performance of Microbial Electrochemical Reduction of CO₂ to Produce Value-Added Chemicals

The electrochemical reduction of CO₂ into value-added chemicals such as formate, methane, acetate, and other multi-carbon compounds (e.g., butyrate, caproate, butanol, ethanol, and PHB) depends on various factors such as applied microorganisms as whole-

cell biocatalysts, electron-generated electrodes, and electron transfer. Various strategies which have been applied to increase the performance of the microbial electrochemical reduction of CO₂ to produce value-added chemicals are depicted in Figure 2. The performance of the electrochemical reduction of CO₂ into value-added chemicals is highly dependent on several factors such as microorganisms as whole-cell biocatalysts, the reactor design, electrode materials and designs, and the reaction conditions (e.g., poised cathode potential, hydraulic retention time). Thus, the modification of electrode materials has shown a good strategy to enhance the performance of the electrochemical reduction of CO₂ to produce various compounds. A wide range of electrode materials such as 3D-G-CF electrodes, Ni-based PHF/CNTs electrodes, and CF/rGO-MNPs enhanced the performance of the electrochemical reduction of CO₂ [37,63,75]. Additionally, diversifying reaction conditions such as the cathode potential for the electrochemical reduction of CO₂ by *Clostridium scatologenes* ATCC 25775T obtained the conditions to have a better performance for the reduction of CO₂ to produce acetate, butyrate, and ethanol [48]. It was reported that diversifying microorganisms as whole-cell biocatalysts showed a diverse performance and range of products for the electrochemical reduction of CO₂. Discovering and applying experimentally various microorganisms as whole-cell biocatalysts for a reaction process to reduce CO₂ is also another good strategy for the enhancement of the reaction. For example, *M. extorquens* AM1 with the best performance toward the reduction of CO₂ was selected for further study from eight *Methylobacterium* species [26]. Another strategy is to optimize the growth medium and conditions to increase the expression level of important enzymes/proteins of microorganisms before applying the microorganism as a whole-cell biocatalyst for the reduction of CO₂. The optimization of the growth media (fumarate, nitrate, and lactate) and conditions (anaerobic and aerobic condition) of *S. oneidensis* MR1, based on the transcriptomic data, was performed in our group to increase the expression level of the enzymes/proteins of the bacteria involved in the electrochemical reduction of CO₂ into formate is an example for the enhancement of the electrochemical reduction of CO₂ into formate. As a result, the reaction rate and final conversion of the reduction of CO₂ into formate catalyzed by *S. oneidensis* MR1, which was grown anaerobically in an optimized LB medium supplemented with fumarate and nitrate as electron receptors and lactate as an electron donor, were remarkably increased compared to those catalyzed by the bacteria which were grown aerobically in a basic LB medium [13]. A recent study on the collaboration of a specialized electron-uptaking microorganism IS4 strain (DSM 15630) and another microorganism capable of producing target value-added chemicals (e.g., *Acetobacterium woodii* for acetate production [61] and *Methanococcus maripaludis* MM901 for methane production [62]) in co-cultures showed a better performance for the electrochemical reduction of CO₂ to produce value-added chemicals. The collaboration of microorganisms (in the form of co-cultures or mixed cultures) would be another good strategy to enhance the performance of the electrochemical reduction of CO₂ to produce value-added chemicals.

Another strategy based on an in silico study (e.g., Basic Local Alignment Searching Tools (BLAST) [95,96] and Clustal program [97]) is introduced in this study to predict potential microorganisms as whole-cell biocatalysts for further experimental verification toward CO₂ reduction. BLAST is a searching tool to compare a query sequence (e.g., nucleotide sequence or amino acid sequence) with a database of sequences and thereby identify sequences that are similar to the query sequence [96]. A Clustal program is used for sequence alignment to find out conserved regions/sites between different sequences [97]. *S. oneidensis* MR1 was selected as the model microorganism for an in silico study to predict a potential microorganism as a whole-cell biocatalyst for the electrochemical reduction of CO₂ into formate. Formate dehydrogenases and electron-transporting proteins (e.g., MtrA, MtrB, MtrC) of *S. oneidensis* MR1, which are important for the electrochemical reduction of CO₂ into formate, were selected as template protein sequences to search for available protein sequences belonging to other microorganisms in the protein sequence database using the BLAST program [95] that are similar to that of *S. oneidensis* MR1 (query sequences

for BLAST are formate dehydrogenase and electron-transporting proteins such as MtrA, MtrB, MtrC of *S. oneidensis* MR1, as seen in Table S1).



Figure 2. Strategies for the enhancement of the electrochemical reduction of CO₂ to produce value-added chemicals.

The BLASTing results, as seen in Table 2, showed that the protein sequences of formate dehydrogenases (subunit alpha1, beta 1, and gamma1 of the FDH_A1B1C1 complex and subunits alpha2, beta2, and gamma2 of the FDH_A2B2C2 complex) have a high similarity with their homologues from other species of the *Shewanella* genus. Formate dehydrogenase subunit alpha1 of *S. oneidensis* MR1 is 74–94% similar to the formate dehydrogenase alpha from 198 other species of the *Shewanella* genus; FDH subunit beta1 and subunit gamma1 of *S. oneidensis* MR1 are also highly similar to their FDH homologues of a respective 173 and 196 other species of the *Shewanella* genus (BLAST identity is 82–89% and 54–98% for FDH subunit beta1 and FDH subunit gamma1, respectively). The BLASTing results, as seen in Table 2, for MtrA, MtrB, and MtrC of *S. oneidensis* MR1 are also highly similar to their homologues from other species of the *Shewanella* genus. The MtrCAB proteins of *S. oneidensis* MR1 are 43–99%, 65–98%, and 32–98% similar to the MtrCAB homolog proteins from a respective 214, 211, and 214 other species of the *Shewanella* genus. The protein sequence alignment of formate dehydrogenase (subunit alpha, beta, and gamma) and the MtrCAB proteins of *S. oneidensis* and their protein homologues from other species of the *Shewanella* genus (*S. oneidensis* MR1, *S. glacialipiscicola*, *S. algae*, *S. litoralis*, *S. woodyi*, and *S. halifaxensis*) are seen in Figures S1–S6. The protein sequence alignment, as seen in Figures S1–S3 and Table 3, showed that the formate dehydrogenase alpha1, beta1, and gamma1 subunits from *S. oneidensis* MR1 are 83–96%, 89–97%, and 56–95% similar to the FDH_alpha_beta_gamma subunits from other species of the *Shewanella* genus. The formate dehydrogenase subunits alpha1, beta1, and gamma 1 of *S. oneidensis* MR1 are highly similar to their homologues from *S. glacialipiscicola*, *S. algae*, and *S. litorali*. On the other hand, the formate dehydrogenase gamma1 of *S. oneidensis* MR1 is moderately similar to its homologue from the two species *S. woodyi* and *S. halifaxensis* (56–66%). The BLAST and protein sequence alignment for the formate dehydrogenase and MtrCAB proteins showed that other species of the *Shewanella* genus possess both formate dehydrogenase and electron-transporting proteins with a diverse similarity in their sequences from moderate to high similarity corresponding protein sequences of *S. oneidensis* MR1. Other *Shewanella* species would be good sources for expanding as whole-cell biocatalysts for the reduction of CO₂ into formic acid. The BLASTing results, as seen in Table 2, also showed that species of *Aeromonas*, *Halomonas*, *Ferrimonas*, and *Vibrio* genera possess both formate dehydroge-

nase and MtrCAB homologues which are relatively high similarity with the query protein sequences of *S. oneidensis* MR1 (32 species of *Aeromonas* genus, 12 species of *Vibrio* genus, 11 species of *Ferrimonas* genus, 1 species of *Halomonas* genus). Bacteria belonging to *Aeromonas*, *Ferrimonas*, *Halomonas*, and *Vibrio* genera would be potential sources for applying as whole-cell biocatalysts for the reduction of CO₂ into formic acid. Table 2 showed that the bacterial species of *Moritella* and *Ralstonia* genera only possess the FDH alpha, beta, and gamma subunits which are relatively high similarity to the formate dehydrogenase subunits from *S. oneidensis* MR1 and do not have any MtrCAB proteins which are similar to that of *S. oneidensis* MR1. The FDH_A1B1C1 subunits of the *Moritella* genus are 66–67%, 77–81%, and 39–40% similar to that of *S. oneidensis* MR1 and the FDH_A1B1C1 subunits of the *Ralstonia* genus are 57–59%, 68–76%, and 37–40% similar to that of *S. oneidensis* MR1. On the other hand, one species of *Geobacter* discovered by the BLAST search (BLOSUM45 and searching in 5000 available protein sequences) has the MtrAB protein which is 32–44% and 22% similar to that of *S. oneidensis* MR1. This finding is similar with the study of Shi et al. on the extracellular electron transfer system of *Geobacter* sp. M21 which contains MtrAB homologues (GM21_0397 and GM21_0398), but no MtrC homologue [98]. The study of Leang et al. showed that *Geobacter sulfurreducens* has *c-type* cytochrome OmcS which has a function as MtrC [99]. Additionally, the genome of *Geobacter sulfurreducens* contains formate dehydrogenase localized in periplasmic. The FDH of *G. sulfurreducens* has four subunits (GSU0777-80). FdnG (GSU07777), which is a catalytic subunit, is more abundant in the hydrogen condition. FdhHG, FdhH, and FdhI exhibited a different abundance in various growth conditions. FdhI is a membrane-associated domain of CbcL that functions as an MQ oxidoreductase [100]. Therefore, bacterial species of *Geobacter* would be another choice for applying as potential whole-cell biocatalysts for the conversion of CO₂ into formate.

Table 2. BLASTing results of formate dehydrogenases and several electron-transporting proteins from *Shewanella oneidensis* MR1 against available sequences in nr protein sequences.

Query Sequences	Organisms Containing Proteins That Are Similar to Corresponding Query Sequences			
	Organism	No. of Organism	BLAST Identity of Protein from Organism with Query Sequence (%)	Classification of the Organism
FDH_alpha1 (genebank accession No.: AAN57473.1)	<i>Shewanella</i> spp.	198	78–94	Gammaproteobactea
	<i>Halomonas</i> spp.	170	63–67	Gammaproteobactea
	<i>Moritella</i> spp.	15	66–67	Gammaproteobactea
	<i>Vibrio</i> spp.	408	67–68	Gammaproteobactea
	<i>Aeromonas</i> spp.	78	67–68	Gammaproteobactea
	<i>Ralstonia</i> spp.	40	57–59	Gammaproteobactea
	<i>Ferrimonas</i> spp.	11	72–78	Gammaproteobactea
	<i>Geobacter</i> spp.	0	-	Gammaproteobactea
FDH_beta1 (genebank accession No.: AAN57474.1)	<i>Shewanella</i> spp.	173	82–89	Gammaproteobactea
	<i>Halomonas</i> spp.	127	69–81	Gammaproteobactea
	<i>Moritella</i> spp.	15	71–88	Gammaproteobactea
	<i>Vibrio</i> spp.	248	68–92	Gammaproteobactea
	<i>Aeromonas</i> spp.	42	80–89	Gammaproteobactea
	<i>Ralstonia</i> spp.	39	68–76	Gammaproteobactea
	<i>Ferrimonas</i> spp.	11	77–79	Gammaproteobactea
	<i>Geobacter</i> spp.	0	-	Gammaproteobactea

Table 2. Cont.

Query Sequences	Organisms Containing Proteins That Are Similar to Corresponding Query Sequences			
	Organism	No. of Organism	BLAST Identity of Protein from Organism with Query Sequence (%)	Classification of the Organism
FDH_gamma1 (genebank accession No.: AAN57475.1)	<i>Shewanella</i> spp.	196	53–99	Gammaproteobactea
	<i>Halomonas</i> spp.	169	39–40	Gammaproteobactea
	<i>Moritella</i> spp.	15	39–40	Gammaproteobactea
	<i>Vibrio</i> spp.	429	36–43	Gammaproteobactea
	<i>Aeromonas</i> spp.	60	39–43	Gammaproteobactea
	<i>Ralstonia</i> spp.	39	37–40	Gammaproteobactea
	<i>Ferrimonas</i> spp.	12	46–57	Gammaproteobactea
	<i>Geobacter</i> spp.	0	-	Deltaproteobactea
FDH_alpha2 (genebank accession No.: AAN57477.1)	<i>Shewanella</i> spp.	198	74–92	Gammaproteobactea
	<i>Halomonas</i> spp.	170	62–63	Gammaproteobactea
	<i>Moritella</i> spp.	15	66–67	Gammaproteobactea
	<i>Vibrio</i> spp.	410	67–69	Gammaproteobactea
	<i>Aeromonas</i> spp.	78	62–65	Gammaproteobactea
	<i>Ralstonia</i> spp.	10	55–57	Gammaproteobactea
	<i>Ferrimonas</i> spp.	11	71–78	Gammaproteobactea
	<i>Geobacter</i> spp.	0	-	Deltaproteobactea
FDH_beta2 (genebank accession No.: AAN57478.1)	<i>Shewanella</i> spp.	173	85–96	Gammaproteobactea
	<i>Halomonas</i> spp.	127	71–79	Gammaproteobactea
	<i>Moritella</i> spp.	15	74–85	Gammaproteobactea
	<i>Vibrio</i> spp.	246	76–91	Gammaproteobactea
	<i>Aeromonas</i> spp.	42	86–87	Gammaproteobactea
	<i>Ralstonia</i> spp.	39	73–74	Gammaproteobactea
	<i>Ferrimonas</i> spp.	11	78–82	Gammaproteobactea
	<i>Geobacter</i> spp.	0	-	Deltaproteobactea
FDH_gamma2 (genebank accession No.: AAN57479.1)	<i>Shewanella</i> spp.	196	53–99	Gammaproteobactea
	<i>Halomonas</i> spp.	169	35–47	Gammaproteobactea
	<i>Moritella</i> spp.	15	35–36	Gammaproteobactea
	<i>Vibrio</i> spp.	428	33–50	Gammaproteobactea
	<i>Aeromonas</i> spp.	60	35–36	Gammaproteobactea
	<i>Ralstonia</i> spp.	38	32–35	Gammaproteobactea
	<i>Ferrimonas</i> spp.	12	54–76	Gammaproteobactea
	<i>Geobacter</i> spp.	0	-	Deltaproteobactea
MtrC (genebank accession No.: AAN54831.1)	<i>Shewanella</i> spp.	214	43–99	Gammaproteobactea
	<i>Halomonas</i> spp.	1	32	Gammaproteobactea
	<i>Moritella</i> spp.	0	-	Gammaproteobactea
	<i>Vibrio</i> spp.	12	24–32	Gammaproteobactea
	<i>Aeromonas</i> spp.	36	24–29	Gammaproteobactea
	<i>Ralstonia</i> spp.	0	-	Gammaproteobactea

Table 2. Cont.

Query Sequences	Organisms Containing Proteins That Are Similar to Corresponding Query Sequences			
	Organism	No. of Organism	BLAST Identity of Protein from Organism with Query Sequence (%)	Classification of the Organism
MtrB (genebank accession No.: AAN54829.1)	<i>Ferrimonas</i> spp.	11	35–42	Gammaproteobactea
	<i>Geobacter</i> spp.	0	-	Deltaproteobactea
	<i>Shewanella</i> spp.	214	32–98	Gammaproteobactea
	<i>Halomonas</i> spp.	3	24–38	Gammaproteobactea
	<i>Moritella</i> spp.	0	-	Gammaproteobactea
	<i>Vibrio</i> spp.	83	25–83	Gammaproteobactea
	<i>Aeromonas</i> spp.	39	27–30	Gammaproteobactea
	<i>Ralstonia</i> spp.	0	-	Gammaproteobactea
	<i>Ferrimonas</i> spp.	12	35–47	Gammaproteobactea
	<i>Geobacter</i> spp.	1	22–24	Deltaproteobactea
MtrA (genebank accession No.: AAN54830.1)	<i>Shewanella</i> spp.	211	65–98	Gammaproteobactea
	<i>Halomonas</i> spp.	3	41–57	Gammaproteobactea
	<i>Moritella</i> spp.	0	-	Gammaproteobactea
	<i>Vibrio</i> spp.	74	45–59	Gammaproteobactea
	<i>Aeromonas</i> spp.	34	48–54	Gammaproteobactea
	<i>Ralstonia</i> spp.	0	-	Gammaproteobactea
	<i>Ferrimonas</i> spp.	12	60–66	Gammaproteobactea
	<i>Geobacter</i> spp.	19	32–46	Deltaproteobactea

Table 3. Similarity (%) between formate dehydrogenases and electron-transporting proteins from *S. oneidensis* MR1 and corresponding enzymes/proteins from several *Shewanella* genus using CLUSTALX2 with BLOSUM62.

Protein/Enzyme from <i>S. oneidensis</i> MR1	Similarity (%) between Formate Dehydrogenase and Electron-Transporting Protein from <i>S. oneidensis</i> MR1 and Its Enzyme/Protein Homolog from Several <i>Shewanella</i> Genus				
	<i>S. glacialipiscicola</i>	<i>S. algae</i>	<i>S. litoralis</i>	<i>S. woodyi</i>	<i>S. halifaxensis</i>
FDH_alpha1	96	94	94	93	83
FDH_beta1	89	99	97	94	89
FHD_gamma1	95	88	85	66	56
MtrA	98	92	84	90	87
MtrB	95	86	80	84	81
MtrC	58	60	65	64	72

5. Conclusions

This study showed the progress in the application of a diversity of microorganisms (pure cultures such as *Shewanella oneidensis* MR1, *Methanobacterium palustre* ATCC BAA-1077, and many strains of *Methylobacterium*, *Sporomusa* genera, *Clostridium* genera, and mixed microbial cultures) as whole-cell biocatalysts for the electrochemical reduction of CO₂ to produce various value-added chemicals, including methane, carboxylates/carboxylic acids (e.g., formate, acetate, butyrate, oxo-butyrate, caproate), alcohols (e.g., ethanol, butanol), and bioplastics (e.g., polyhydroxybutyrate). The performance of the microbial electrochemical reduction of CO₂ to produce formate and acetate is significantly increased

by applying a diversity of microorganisms (e.g., *Shewanella oneidensis* MR1 and several strains of *Methylobacterium* for formate production or several strains of *Sporomusa* genera for acetate production), the modification of electrode materials, the power of the electrode supply in the study of acetate production by *Sporomusa ovata* DSM 2662 and enhancing the catalytic efficiency of *Shewanella oneidensis* MR1 through optimizing the growth medium and conditions to increase the expression level of the involved proteins/enzymes such as formate dehydrogenase and MtrABC cytochromes of *Shewanella oneidensis* MR1. Some recent studies showed the capability of microorganisms as whole-cell biocatalysts for a longer chain of higher value-added chemicals such as n-butyrate and n-caproate. Additionally, this study also provided several examples of influential factors including the electrode materials, the power of the electron supply, the electron mediator, and the diversity of microorganisms as whole-cell biocatalysts on the performance of the microbial electrochemical reduction of CO₂. Combining the diversity of microorganisms as whole-cell biocatalysts with other influential factors such as the electrode materials and power of the electron supply would be a good choice to obtain a better performance of the electrochemical reduction of CO₂ to produce value-added chemicals. Remarkably, this study provided insights, at a molecular level, of the involved enzymes/proteins of the microorganisms to elucidate how the microorganisms, such as *M. extorsquens* AM1, *S. oneidensis* MR1, and *Sporomusa ovata*, play a role as whole-cell biocatalysts for the electrochemical reduction of CO₂ to produce value-added chemicals. Additionally, this study provides several strategies which have been applied to enhance the performance of the reduction of CO₂ such as the experimental screening of microorganisms as whole-cell biocatalysts, the optimization of the growth medium and conditions of the microorganism before applying the reduction system based on the genomic and transcriptomic analysis of the microorganisms and a strategy based on an in silico study to predict the potential microorganism as a whole-cell biocatalyst in this study. This study, based on an in silico study, also provides a list of microorganisms belonging to the *Shewanella* genus, *Aeromonas*, *Halomonas*, *Ferrimonas*, *Vibrio*, and *Geobacter* which would be the candidates as whole-cell biocatalysts for the reduction of CO₂ to produce value-added chemicals.

Supplementary Materials: The following supporting information can be downloaded at: <https://www.mdpi.com/article/10.3390/pr11030766/s1>, Table S1: List of proteins/enzymes from *S. oneidensis* MR1 obtained from NCBI (<https://www.ncbi.nlm.nih.gov/>) (accessed on 15 June 2022 for MtrCAB (MtrC, MtrA, MtrB) sequences and 16 June 2022 for FDH sequences, respectively) and used for screening potential whole-cell biocatalysts by Basic Local Alignment Searching Tools (BLAST); Figure S1: Protein sequence alignment of formate dehydrogenase subunit alpha from *S. oneidensis* MR1 (Genbank Accession no. AAN57473.1), *S. glacialipiscicola* (Genbank accession no. WP_220772316.1), *S. algae* (Genbank accession no. WP_208160371.1), *S. litoralis* (WP_160055551.1), *S. woodyi* (Genbank accession no. WP_012327379.1), and *S. halifaxensis* (WP_108944961.1); Figure S2: Protein sequence alignment of formate dehydrogenase subunit beta from *S. oneidensis* MR1 (Genbank Accession no. AAN57474.1), *S. glacialipiscicola* (Genbank accession no. WP_220772313.1), *S. algae* (Genbank accession no. WP_144226586.1), *S. litoralis* (WP_160055427.1), *S. woodyi* (Genbank accession no. WP_012327378.1), and *S. halifaxensis* (WP_108944958.1); Figure S3: Protein sequence alignment of formate dehydrogenase subunit gamma from *S. oneidensis* MR1 (Genbank Accession no. AAN57475.1), *S. glacialipiscicola* (Genbank accession no. WP_220772315.1), *S. algae* (Genbank accession no. WP_219031328.1), *S. litoralis* (Genbank accession no. WP_160055429.1), *S. woodyi* (Genbank accession no. WP_065204495.1), and *S. halifaxensis* (genbank accession no. WP_012279080.1); Figure S4: Protein sequence alignment of MtrA from *S. oneidensis* MR1 (Genbank Accession no. AAN54830.1), *S. glacialipiscicola* (Genbank accession no. WP_220772614.1), *S. algae* (Genbank accession no. WP_208149284.1), *S. litoralis* (Genbank accession no. WP_160053383.1), *S. woodyi* (Genbank accession no. WP_012325733.1), and *S. halifaxensis* (genbank accession no. WP_012277866.1); Figure S5: Protein sequence alignment of MtrB from *S. oneidensis* MR1 (Genbank Accession no. AAN54829.1), *S. glacialipiscicola* (Genbank accession no. WP_220772616.1), *S. algae* (Genbank accession no. WP_159353283.1), *S. litoralis* (Genbank accession no. WP_160053384.1), *S. woodyi* (Genbank accession no. WP_065188554.1), and *S. halifaxensis* (genbank accession no. WP_012277867.1);

Figure S6: Protein sequence alignment of MtrC from *S. oneidensis* MR1 (Genbank Accession no. AAN54831.1), *S. glacialipiscicola* (Genbank accession no. WP_220772613.1), *S. algae* (Genbank accession no. WP_234523060.1), *S. litoralis* (Genbank accession no. WP_160053382.1), *S. woodyi* (Genbank accession no. WP_065188553.1), and *S. halifaxensis* (genbank accession no. WP_108946855.1).

Funding: This research is funded by Ho Chi Minh City Open University under the grant number E2019.04.1.

Data Availability Statement: Not Applicable.

Acknowledgments: We wish to express our thanks to the research project sponsored by Ho Chi Minh City Open University, Ho Chi Minh City, Vietnam.

Conflicts of Interest: The author declares no conflict of interest.

References

- Ekwurzel, B.; Boneham, J.; Dalton, M.W.; Heede, R.; Mera, R.J.; Allen, M.R.; Frumhoff, P.C. The rise in global atmospheric CO₂, surface temperature, and sea level from emissions traced to major carbon producers. *Clim. Chang.* **2017**, *144*, 590–2017. [CrossRef]
- Yoro, O.K.; Daramola, O.M. CO₂ emission sources, greenhouse gases, and the global warming effect. In *Advances in Carbon Capture Methods*; Woodhead Publishing: Sawston, UK, 2020; pp. 3–28.
- Fawzy, S.; Osman, A.I.; Doran, J.; Rooney, D.W. Strategies for mitigation of climate change: A review. *Environ. Chem. Lett.* **2020**, *18*, 2069–2094. [CrossRef]
- Al-Mamoori, A.; Krishnamurthy, A.; Rownaghi, A.A.; Rezaei, F. Carbon Capture and Utilization Update. *Energy Technol.* **2017**, *5*, 834–849. [CrossRef]
- Dowell, N.M.; Fennell, P.S.; Shah, N.; Maitland, G.C. The role of CO₂ capture and utilization in mitigating climate change. *Nat. Clim. Chang.* **2017**, *7*, 243–249. [CrossRef]
- Anwar, M.; Fayyaz, A.; Sohail, N.; Khokhar, M.; Baqar, M.; Yasar, A.; Rasool, K.; Nazir, A.; Raja, M.; Rehan, M.; et al. CO₂ utilization: Turning greenhouse gas into fuels and valuable products. *J. Environ. Manage.* **2020**, *260*, 110059. [CrossRef]
- Qureshi, F.; Yusuf, M.; Kamyab, H.; Zaidi, S.; Khalil, M.J.; Khan, M.A.; Alam, M.A.; Masood, F.; Bazil, L.; Chelliapan, S.; et al. Current trends in hydrogen production, storage and applications in India: A review. *Sust. Energy Technol. Assess.* **2022**, *53*, 102677. [CrossRef]
- Qureshi, F.; Yusuf, M.; Kamyab, H.; Vo, D.-V.N.; Chelliapan, S.; Joo, S.-W.; Vasseghian, Y. Latest eco-friendly avenues on hydrogen production towards a circular bioeconomy: Currents challenges, innovative insights, and future perspectives. *Renew. Sustain. Energy Rev.* **2022**, *168*, 112916. [CrossRef]
- Dawood, F.; Anda, M.; Shafiullah, G.M. Hydrogen production for energy: An overview. *Int. J. Hydrog. Energy* **2020**, *45*, 3847–3869. [CrossRef]
- Finn, C.; Schnittger, S.; Yellowlees, L.; Love, J. Molecular approaches to the electrochemical reduction of carbon dioxide. *Chem. Comm.* **2012**, *48*, 1392–1399. [CrossRef]
- Langanke, J.; Wolf, A.; Hofmann, J.; Bohm, K.; Subhani, M.; Muller, T.; Leitner, W.; Gurtler, C. Carbon dioxide (CO₂) as sustainable feedstock for polyurethane production. *Green Chem.* **2014**, *16*, 1864–1870. [CrossRef]
- Iqbal, F.; Abdullah, B.; Oladipo, H.; Yusuf, M.; Alenazey, F.; Nguyen, T.D.; Ayou, M. Recent developments in photocatalytic irradiation from CO₂ to methanol. In *Nanostructured Photocatalysts- from Fundamental to Practical Applications*; Nguyen, V., Vo, D.N., Nanda, S., Eds.; Elsevier: Amsterdam, The Netherlands, 2021; pp. 519–540.
- Le, Q.A.T.; Kim, H.G.; Kim, Y.H. Electrochemical synthesis of formic acid from CO₂ catalyzed by *Shewanella oneidensis* MR-1 whole-cell biocatalyst. *Enzym. Microb. Technol.* **2018**, *116*, 5–2018. [CrossRef]
- Ganigué, R.; Puig, S.; Batlle-Vilanova, P.; Balaguera, M.D.; Colprima, J. Microbial electrosynthesis of butyrate from carbon dioxide. *Chem. Commun.* **2015**, *51*, 3235–3238. [CrossRef] [PubMed]
- Pillot, G.; Sunny, S.; Comes, V.; Kerzenmacher, S. Optimization of growth and electrosynthesis of PolyHydroxyAlkanoates by the thermophilic bacterium *Kyrpidia spormannii*. *Bioresour. Technol. Rep.* **2022**, *17*, 100949. [CrossRef]
- Zaybak, Z.; Pisciotta, J.M.; Tokash, J.C.; Logan, B.E. Enhanced start-up of anaerobic facultatively autotrophic biocathodes in bioelectrochemical systems. *J. Biotechnol.* **2013**, *168*, 478–485. [CrossRef] [PubMed]
- Schuchmann, K.; Muller, V. Direct and reversible hydrogenation of CO₂ to formate by bacterial carbon dioxide reductase. *Science* **2013**, *342*, 1382–1385. [CrossRef]
- Alissandratos, A.; Kim, H.K.; Easton, C. Formate production through carbon dioxide hydrogenation with recombinant whole cell biocatalysts. *Bioresour. Technol.* **2014**, *164*, 11–2014. [CrossRef]
- Rowe, S.F.G.L.; Ainsworth, E.V.; Davies, J.A.; Lockwood, C.W.J.; Shi, L.; Elliston, A.; Roberts, I.N.; Waldron, K.W.; Richardson, D.J.; Clarke, T.A.; et al. Light-Driven H₂ Evolution and C=C or C=O Bond Hydrogenation by *Shewanella oneidensis*: A Versatile Strategy for Photocatalysis by Nonphotosynthetic Microorganisms. *ACS Catal.* **2017**, *7*, 7558–7566. [CrossRef]
- Alissandratos, A.; Easton, C.J. Biocatalysis for the application of CO₂ as a chemical feedstock. *Beilstein J. Org. Chem.* **2015**, *11*, 2370–2387. [CrossRef]
- Marpani, F.; Pinelo, M.; Meyer, A.S. Enzymatic conversion of CO₂ to CH₃OH via reverse dehydrogenase cascade biocatalysis: Quantitative comparison of efficiencies of immobilized enzyme systems. *Biochem. Eng. J.* **2017**, *127*, 228–2017. [CrossRef]

22. Choe, H.; Joo, J.; Kim, M.; Lee, S.; Jung, K.; Kim, Y. Efficient CO₂-reducing activity of NAD-dependent formate dehydrogenase from *Thiobacillus* sp. KNK65MA for formate production from CO₂ gas. *PLoS ONE* **2014**, *9*, e10311. [[CrossRef](#)] [[PubMed](#)]
23. Hartmann, T.; Leimkühler, S. The oxygen-tolerant and NAD⁺-dependent formate dehydrogenase from *Rhodobacter capsulatus* is able to catalyze the reduction of CO₂ to formate. *FEBS J.* **2013**, *280*, 6083–6096. [[CrossRef](#)] [[PubMed](#)]
24. Luo, J.; Meyer, S.A.; Mateiu, R.V.; Pinolo, M. Cascade catalysis in membranes with enzyme immobilization for multi-enzymatic conversion of CO₂ to methanol. *New Biotechnol.* **2015**, *32*, 319–327. [[CrossRef](#)] [[PubMed](#)]
25. Cazelles, R.; Drone, J.; Fajula, F.; Ersen, O.; Moldovan, S.; Galarneau, A. Reduction of CO₂ to methanol by a polyenzymatic system encapsulated in phospholipids–silica nanocapsules. *New J. Chem.* **2013**, *37*, 3721. [[CrossRef](#)]
26. Hwang, H.; Yeon, Y.; Lee, S.; Choe, H.; Cho, D.; Park, S.; Kim, Y. Electro-biocatalytic production of formate from carbon dioxide using an oxygen-stable whole-cell biocatalyst. *Bioresour. Technol.* **2015**, *185*, 35–39. [[CrossRef](#)]
27. Srikanth, S.; Maesen, M.; Dominguez-Benetton, X.; Vanbroekhoven, K.; Pant, D. Enzymatic electrosynthesis of formate through CO₂ sequestration/reduction in a bioelectrochemical system (BES). *Bioresour. Technol.* **2014**, *165*, 350–354. [[CrossRef](#)]
28. Lienemann, M.; Deutzmann, J.S.; Milton, R.D.; Sahin, M.; Spormann, A.M. Mediator-free enzymatic electrosynthesis of formate by the *Methanococcus maripaludis* heterodisulfide reductase supercomplex. *Bioresour. Technol.* **2018**, *254*, 278–283. [[CrossRef](#)]
29. Cheng, S.; Call, X.D.F.D.; Logan, E.B. Direct Biological Conversion of Direct Biological Conversion of Direct Biological Conversion of. *Environ. Sci. Technol.* **2009**, *43*, 3953–3958. [[CrossRef](#)]
30. Lohner, S.T.; Deutzmann, J.S.; Logan, B.E.; Spormann, A.M. Hydrogenase-independent uptake and metabolism of electrons by the archaeon *Methanococcus maripaludis*. *ISME J.* **2014**, *8*, 1673–1681. [[CrossRef](#)]
31. Schlager, S.; Dumitru, L.M.; Haberbauer, M.; Fuchsbauer, A.; Neugebauer, H.; Hiemetsberger, D.; Wagner, A.; Portenkirchner, E.; Sariciftci, N.S. Electrochemical Reduction of Carbon Dioxide to Methanol by Direct Injection of Electrons into Immobilized Enzymes on a Modified Electrode. *ChemSusChem* **2016**, *9*, 631–635. [[CrossRef](#)]
32. Aryal, N.; Tremblay, P.-L.; Lizak, M.D.; Zhang, T. Performance of different *Sporomusa* species for the microbial electrosynthesis of acetate from carbon dioxide. *Bioresour. Technol.* **2017**, *233*, 184–190. [[CrossRef](#)]
33. Nevin, P.K.; Hensley, A.S.; Franks, E.; Summers, M.; Ou, J.; Woodard, L.T.; Snoeyenbos-West, L.; Lovley, R.D. Electrosynthesis of organic compounds from Carbon dioxide is catalyzed by a diversity of acetogenic microorganism. *Appl. Environ. Microbiol.* **2011**, *77*, 2882–2886. [[CrossRef](#)] [[PubMed](#)]
34. Yuan, M.; Kummer, J.M.; Minter, D.S. Strategies for bioelectrochemical CO₂ reduction. *Chem. Eur. J.* **2019**, *25*, 14258–14266. [[CrossRef](#)] [[PubMed](#)]
35. Chiranjeevi, P.; Bulut, M.; Patil, B.T.S.A.; Pant, D. Current trends in enzymatic electrosynthesis for CO₂ reduction. *Curr. Opin. Green Sustain. Chem.* **2019**, *16*, 65–70. [[CrossRef](#)]
36. Rabaey, K.; Rozendal, R.A. Microbial electrosynthesis—Revisiting the electrical route for microbial production. *Nat. Rev. Microbiol.* **2010**, *8*, 706–716. [[CrossRef](#)] [[PubMed](#)]
37. Bian, B.; Alqahtani, F.M.; Katuri, P.K.; Liu, D.; Bajracharya, S.; Lai, Z.; Rabaey, K.; Saikaly, E.P. Porous nickel hollow fiber cathodes coated with CNTs for efficient microbial electrosynthesis of acetate from CO₂ using *Sporomusa ovata*. *J. Mater. Chem. A* **2018**, *6*, 17201–17211. [[CrossRef](#)]
38. Nevin, K.P.; Woodard, T.L.; Franks, A.E.; Summers, Z.M.; Lovley, D.R. Microbial Electrosynthesis: Feeding Microbes Electricity to Convert Carbon Dioxide and Water to Multicarbon Extracellular Organic compounds. *mBio* **2010**, *1*, e00103-10. [[CrossRef](#)]
39. Karthikeyan, R.; Singh, R.; Bose, A. Microbial electron uptake in microbial electrosynthesis: A mini-review. *J. Ind. Microbiol. Biotechnol.* **2019**, *46*, 1419–1426. [[CrossRef](#)]
40. Tremblay, P.-L.; Faraghiparapari, N.; Zhang, T. Accelerated H₂ Evolution during Microbial Electrosynthesis with *Sporomusa ovata*. *Catalysts* **2019**, *9*, 166–176. [[CrossRef](#)]
41. Igarashi, K.; Kato, S. Extracellular electron transfer in acetogenic bacteria and its application for conversion of carbon dioxide into organic compounds. *Appl. Microbiol. Biotechnol.* **2017**, *101*, 6301–6307. [[CrossRef](#)]
42. Chen, L.; Tremblay, P.-L.; Mohanty, S.; Xu, K.; Zhang, T. Electrosynthesis of acetate from CO₂ by a highly structured biofilm assembled with reduced graphene oxide–tetraethylene pentaamine. *J. Mater. Chem. A* **2016**, *4*, 8395–8401. [[CrossRef](#)]
43. Zhang, T.; Nie, H.; Bain, S.T.; Lu, H.; Cui, M.; Snoeyenbos-West, L.O.; Franks, E.A.; Nevin, P.K.; Lovley, R.D. Improved cathode materials for microbial electrosynthesis. *Energy Environ. Sci.* **2013**, *6*, 217–224. [[CrossRef](#)]
44. Su, M.; Jang, Y.; Li, D. Production of acetate from Carbon dioxide in biochemical systems based on autotrophic mixed culture. *J. Microbiol. Biotechnol.* **2013**, *23*, 1140–1146. [[CrossRef](#)] [[PubMed](#)]
45. Mayer, F.; Enzmann, F.L.A.M.; Holtmann, D. Performance of different methanogenic species for the microbial electrosynthesis of methane from carbon dioxide. *Bioresour. Technol.* **2019**, *289*, 121706. [[CrossRef](#)]
46. Bajracharya, S.; Krige, A.; Matsakas, L.; Rova, U.; Christakopoulos, P. Advances in cathode designs and reactor configurations of microbial electrosynthesis systems to facilitate gas electro-fermentation. *Bioresour. Technol.* **2022**, *354*, 127178. [[CrossRef](#)] [[PubMed](#)]
47. Li, S.; Song, E.; Baek, J.; Im, S.H.; Sakuntala, M.; Kim, M.; Park, C.; Min, B.; Kim, R.J. Bioelectrosynthetic Conversion of CO₂ Using Different Redox Mediators: Electron and Carbon Different Redox Mediators: Electron and Carbon. *Energies* **2020**, *13*, 2572. [[CrossRef](#)]
48. Liu, H.; Song, T.; Fei, K.; Wang, H.; Xie, J. Microbial electrosynthesis of organic chemicals from CO₂ by *Clostridium scatologenes* ATCC 25775T. *Bioresour. Bioprocess.* **2018**, *5*, 7. [[CrossRef](#)]
49. Jang, J.; Wook, B.; Kim, Y.H. Bioelectrochemical conversion of CO₂ to value added product formate using engineered *Methylobacterium extorquens*. *Sci. Rep.* **2018**, *8*, 7211. [[CrossRef](#)]

50. Rengasamy, K.; Ranaivoarisoa, T.; Bai, W.; Bose, A. Magnetite nanoparticle anchored graphene cathode enhances microbial electrosynthesis of polyhydroxybutyrate by *Rhodospseudomonas palustris* TIE-1. *Nanotechnology* **2021**, *035103*, 32. [[CrossRef](#)]
51. Aryal, N.; Halder, A.; Tremblay, P.-L.; Chi, Q.; Zhang, T. Enhanced microbial electrosynthesis with three-dimensional graphene functioned cathodes fabricated via solvothermal synthesis. *Electrochem. Acta* **2016**, *217*, 117–122. [[CrossRef](#)]
52. Xiang, H.; Miller, H.A.; Bellini, M.; Christensen, H.; Scott, K.; Rasul, S.; Yu, E.H. Production of formate from CO₂ electrochemical reduction and its application in energy storage. *Sustain. Energy Fuels* **2020**, *4*, 277–284. [[CrossRef](#)]
53. Vo, T.; Purohit, K.; Nguyen, C.; Biggs, B.; Mayoral, S.; Haan, J.L. Formate: An Energy Storage and Transport Bridge between Carbon Dioxide and a Formate Fuel Cell in a Single Device. *ChemSusChem* **2015**, *8*, 3853–3858. [[CrossRef](#)]
54. Chistoserdova, L.; Laukel, M.; Portais, J.; Vorholt, A.; Lidstrom, E.M. Multiple Formate Dehydrogenase Enzymes in the Facultative Methylotroph *Methylobacterium extorquens* AM1 Are Dispensable for Growth on Methanol. *J. Bacteriol.* **2004**, *186*, 22–28. [[CrossRef](#)] [[PubMed](#)]
55. Reda, T.; Abram, P.C.N.; Hirst, J. Reversible interconversion of carbon dioxide and formate by an electroactive enzyme. *Proc. Natl. Acad. Sci. USA* **2008**, *105*, 10654–10658. [[CrossRef](#)] [[PubMed](#)]
56. Seelajaroen, H.; Haberbauer, M.; Hemmelmaier, C.; Aljabour, A.; Dumitru, L.M.; Hassel, A.W.; Sariciftci, N.S. Enhanced Bio-Electrochemical Reduction of Carbon Dioxide by Using Neutral Red as a Redox Mediator. *ChemBioChem* **2019**, *20*, 1196–1205. [[CrossRef](#)] [[PubMed](#)]
57. Fredrickson, J.; Romine, M.; Beliaev, A.; Auchtung, J.; Driscoll, M.; Gardner, T.; Nealson, K.; Osterman, A.; Pinchuk, G.; Reed, J.; et al. Towards environmental systems biology of *Shewanella*. *Nat. Rev. Microbiol.* **2008**, *6*, 592–603. [[CrossRef](#)]
58. Logan, B. Exoelectrogenic bacteria that power microbial fuel cells. *Nat. Rev. Microbiol.* **2009**, *7*, 375–381. [[CrossRef](#)]
59. Heidelberg, J.F.; Paulsen, I.T.; Nelson, K.E.; Gaidos, E.J.; Nelson, W.C.; Read, T.D.; Eisen, J.A.; Seshadri, R.; Ward, N.; Methe, B.; et al. Genome sequence of the dissimilatory metal ion-reducing bacterium *Shewanella oneidensis*. *Nature Biotechnol.* **2002**, *20*, 1118–1123. [[CrossRef](#)]
60. Schlager, S.; Haberbauer, M.; Fuchsbaumer, A.; Hemmelmaier, C.; Dumitru, M.L.; Hinterberger, G.; Neugebauer, H.; Sariciftci, S.N. Bio-Electrocatalytic Application of Microorganisms for Carbon Dioxide Reduction to Methane. *ChemSusChem* **2017**, *10*, 226–233. [[CrossRef](#)]
61. Deutzmann, J.S.; Spormann, A.M. Enhanced microbial electrosynthesis by using defined co-cultures. *ISME J.* **2017**, *11*, 704–714. [[CrossRef](#)]
62. Enning, D.; Venzlaff, H.; Garrelfs, J.; Dinh, H.T.; Meyer, V.; Mayrhofer, K.; Hassel, A.W.; Stratmann, M.; Widdel, F. Marine sulfate-reducing bacteria cause serious corrosion of iron under electroconductive biogenic mineral crust. *Environ. Microbiol.* **2012**, *14*, 1772–1787. [[CrossRef](#)]
63. Song, H.; Choi, O.; Pandey, A.; Kim, Y.G.; Joo, J.S.; Sang, B. Simultaneous production of methane and acetate by thermophilic mixed culture from carbon dioxide in bioelectrochemical system. *Bioresour. Technol.* **2019**, *281*, 474–479. [[CrossRef](#)] [[PubMed](#)]
64. Alqahtani, M.F.; Katuri, K.; Bajracharya, S.; Yu, Y.; Lai, Z.; Saikaly, P. Porous Hollow Fiber Nickel Electrodes for Effective Supply and Reduction of Carbon Dioxide to Methane through Microbial Electrosynthesis. *Adv. Funct. Mater.* **2018**, *28*, 1804860. [[CrossRef](#)]
65. Jabari, L.; Gannoun, H.; Cayol, J.-L.; Hamdi, M.; Ollivier, B.; Fauque, G.; Fardeau, M.-L. *Desulfotomaculum peckii* sp. nov., a moderately thermophilic member of the genus *Desulfotomaculum*, isolated from an upflow anaerobic filter treating abattoir wastewaters. *Int. J. Syst. Evol. Microbiol.* **2013**, *63*, 2082–2087. [[CrossRef](#)]
66. Vassilev, I.; Hernandez, P.A.; Battle-Vilanova, P.; Freguia, S.; Krömer, J.O.; Keller, J.; Ledezma, P.; Viridis, B. Microbial Electrosynthesis of Isobutyric, Butyric, Caproic Acids, and Corresponding Alcohols from Carbon Dioxide. *ACS Sustainable Chem. Eng.* **2018**, *6*, 8485–8493. [[CrossRef](#)]
67. Daniell, J.; Köpke, M.; Simpson, S.D. Commercial Biomass Syngas Fermentation. *Energies* **2012**, *5*, 5372–5417. [[CrossRef](#)]
68. Khor, W.C.; Andersen, S.; Vervaeren, H.; Rabaey, K. Electricity-assisted production of caproic acid from grass. *Biotechnol. Biofuels* **2017**, *10*, 180. [[CrossRef](#)]
69. Chen, W.S.; Strik, D.P.; Buisman, C.J.; Kroeze, C. Production of Caproic Acid from Mixed Organic Waste: An Environmental Life Cycle Perspective. *Environ. Sci. Technol.* **2017**, *51*, 7159–7168. [[CrossRef](#)]
70. Kucek, L.A.; Nguyen, M.; Angenent, L.T. Conversion of L-lactate into n-caproate by a continuously fed reactor microbiome. *Water Res.* **2016**, *93*, 163–171. [[CrossRef](#)]
71. Reddy, M.V.; Mohan, S.V.; Chang, Y.-C. Medium-Chain Fatty Acids (MCFA) Production Through Anaerobic Fermentation Using *Clostridium* Through Anaerobic Fermentation Using *Clostridium*. *Appl. Biochem. Biotechnol.* **2018**, *185*, 594–605. [[CrossRef](#)]
72. Moon, J.; Dönig, J.; Kramer, S.; Poehlein, A.; Daniel, R.; Müller, V. Formate metabolism in the acetogenic bacterium *Acetobacterium woodii*. *Environ. Microbiol.* **2021**, *23*, 4214–4227. [[CrossRef](#)]
73. Brown, B.; Wilkins, M.; Saha, R. *Rhodospseudomonas palustris*: A biotechnology chassis. *Biotechnol. Adv.* **2022**, *60*, 108001. [[CrossRef](#)] [[PubMed](#)]
74. Bose, A.; Gardel, E.J.; Vidoudez, C.; Parra, E.A.; Girguis, P.R. Electron uptake by iron-oxidizing phototrophic bacteria. *Nature Commun.* **2014**, *5*, 3391. [[CrossRef](#)]
75. Jourdin, L.; Winkelhorst, M.; Rawls, B.; Buisman, J.S.D.P. Enhanced selectivity to butyrate and caproate above acetate in continuous bioelectrochemical chain elongation from CO₂: Steering with CO₂ loading rate and hydraulic retention time. *Bioresour. Technol. Reports* **2019**, *7*, 100284. [[CrossRef](#)]

76. Arends, J.B.A.; Patil, S.A.; Roume, H.; Rabae, K. Continuous long-term electricity-driven bioproduction of carboxylates and isopropanol from CO₂ with a mixed microbial community. *J. CO₂ Util.* **2017**, *20*, 141–149. [[CrossRef](#)]
77. Aryal, N.; Wan, L.; Overgaard, M.H.; Stoot, A.C.; Chen, Y.; Tremblay, P.-L.; Zhang, T. Increased carbon dioxide reduction to acetate in a microbial electrosynthesis reactor with a reduced graphene oxide-coated copper foam composite cathode. *Bioelectrochemistry* **2019**, *128*, 83–93. [[CrossRef](#)] [[PubMed](#)]
78. Wang, G.; Huang, Q.; Song, T.-S.; Xie, J. Enhancing Microbial Electrosynthesis of Acetate and Butyrate from CO₂ Reduction Involving Engineered *Clostridium ljungdahlii* with a Nickel-Phosphide-Modified Electrode. *Energy Fuels* **2020**, *34*, 8666–8675. [[CrossRef](#)]
79. Amao, Y. Formate dehydrogenase for CO₂ utilization and its application. *J. CO₂ Util.* **2018**, *26*, 623–641. [[CrossRef](#)]
80. Laukel, M.; Chistoserdova, L.; Lidstrom, E.M.; Vorholt, A.J. The tungsten-containing formate dehydrogenase from *Methylobacterium extorquens* AM1: Purifications and properties. *Eur. J. Biochem.* **2003**, *270*, 325–333. [[CrossRef](#)]
81. Edwards, J.M.; White, F.G.; Norman, M.; Tome-Fernandez, A.; Ainsworth, E.; Shi, L.; Fredrickson, K.J.; Zachara, M.J.; Butt, N.J.; Richardson, J.D.; et al. Extracellular decaheme proteins involved in microbe-mineral electron transfer. *Sci. Rep.* **2014**, *5*, 11677. [[CrossRef](#)]
82. Myers, C.; Myers, J. The outer membrane cytochromes of *Shewanella oneidensis* MR-1 are lipoproteins. *Lett. Appl. Microbiol.* **2004**, *39*, 466–470. [[CrossRef](#)]
83. Beliaev, A.S.; Thompson, D.K.; Khare, T.; Lim, H.; Brandt, C.C.; Li, G.; Murray, A.E.; Heidelberg, J.F.; Giometti, C.S.; Yates III, J.; et al. Gene and Protein Expression Profiles of *Shewanella oneidensis* during Anaerobic Growth with Different Electron Acceptors. *MICS A J. Integr. Biol.* **2002**, *6*, 39–60. [[CrossRef](#)]
84. Liu, Y.; Whitman, B.W. Metabolic, phylogenetic, and ecological diversity of the methanogenic Archaea. *Ann. N. Y. Acad. Sci.* **2008**, *1125*, 171–189. [[CrossRef](#)]
85. Ljungdahl, G.L.; Adams, W.M.; Barton, L.L.; Ferry, G.; Johnson, K. *Biochemistry and Physiology of Anaerobic Bacteria*; Springer: New York, NY, USA, 2003.
86. Wongnate, T.; Sliwa, D.; Ginovska, B.; Smith, D.; Wolf, W.M.; Lehnert, N.; Rauegi, S.; Ragsdale, W.S. The radical mechanism of biological methane synthesis by methyl coenzyme M reductase. *Science* **2016**, *352*, 953–958. [[CrossRef](#)] [[PubMed](#)]
87. Bajracharya, S.; Ter Heijne, A.; Benetton, D.X.; Vanbroekhoven, K.; Buisman, J.; Strick, P.D.; Pant, D. Carbon dioxide reduction by mixed and pure cultures in microbial electrosynthesis using an assembly of graphite felt and stainless steel as a cathode. *Bioresour. Technol.* **2015**, *195*, 14–24. [[CrossRef](#)] [[PubMed](#)]
88. Poehlein, A.; Schmidt, S.; Kaster, A.K.; Goenrich, M.; Vollmers, J.; Thürmer, A.; Bertsch, J.; Schuchmann, K.; Voigt, B.; Hecker, M.; et al. An ancient pathway combining carbon dioxide fixation with the generation and utilization of a sodium ion gradient for ATP synthesis. *PLoS ONE* **2012**, *7*, e33439. [[CrossRef](#)]
89. Visser, M.; Pieterse, M.M.; Pinkse, W.M.; Nijssse, B.; Verhaert, D.P.; Vos, M.d.W.; Schaap, J.; Stams, J.A. Unravelling the one-carbon metabolism of the acetogen *Sporomusa* strain An4 by genome and proteome analysis. *Environ. Microbiol.* **2016**, *18*, 2843–2855. [[CrossRef](#)]
90. Rosenbaum, F.; Müller, V. Energy conservation under extreme energy limitation: The role of cytochromes and quinones in acetogenic bacteria. *Extremophiles* **2021**, *25*, 413–424. [[CrossRef](#)] [[PubMed](#)]
91. Ammam, F.; Tremblay, P.-L.; Lizak, M.D.; Zhang, T. Effect of tungstate on acetate and ethanol production by the electrosynthetic bacterium *Sporomusa ovata*. *Biotechnol. Biofuels* **2016**, *9*, 163. [[CrossRef](#)]
92. Spirito, C.M.; Richter, H.; Rabaey, K.; Stams, A.J.A.L.T. Chain elongation in anaerobic reactor microbiomes to recover resources from waste. *Curr. Opin. Biotechnol.* **2014**, *27*, 115–122. [[CrossRef](#)]
93. Joshi, S.; Robles, A.; Aguiar, S.; Delgado, A.G. The occurrence and ecology of microbial chain elongation of carboxylates in soils. *ISME J.* **2021**, *15*, 1907–1918. [[CrossRef](#)]
94. Angenent, L.T.; Richter, H.; Buckel, W.; Spirito, C.M.; Steinbusch, K.J.J.; Plugge, C.M.; Strik, D.P.B.T.B.; Grootscholten, T.I.M.; Buisman, C.J.N.; Hamelers, H.V.M. Chain Elongation with Reactor Microbiomes: Open-Culture Biotechnology to Produce Biochemicals. *Environ. Sci. Technol.* **2016**, *50*, 2796–2810. [[CrossRef](#)]
95. Altschul, F.S.; Gish, W.; Miller, W.; Myers, W.; Lipman, J.D. Basic Local Alignment Search Tool. *J. Mol. Biol.* **1990**, *215*, 403–410. [[CrossRef](#)]
96. Donkor, E.S.; Dayie, N.T.K.D.; Adiku, T.K. Bioinformatics with basic local alignment search tool (blast) and fast alignment (fasta). *J. Bioinform. Seq. Anal.* **2014**, *6*, 1–6.
97. Chenna, R.; Sugawara, H.; Koike, T.; Lopez, R.; Gibson, T.; Higgins, D.; Thompson, J. Multiple sequence alignment with the Clustal series of programs. *Nucleic Acid. Res.* **2003**, *31*, 3497–3500. [[CrossRef](#)] [[PubMed](#)]
98. Shi, L.; Zachara, R.M.M.; Fredrickson, K. Mtr extracellular electron-transfer pathways in Fe(III)-reducing or Fe(II)-oxidizing bacteria: A genomic perspective. *Biochem. Soc. Trans.* **2012**, *40*, 1261–1267. [[CrossRef](#)] [[PubMed](#)]
99. Leang, C.; Qian, X.; Mester, T.; Lovley, D.R. Alignment of the c-Type Cytochrome OmC5 along Pili of *Geobacter sulfurreducens*. *Appl. Environ. Microbiol.* **2010**, *76*, 4080–4084. [[CrossRef](#)] [[PubMed](#)]
100. Mollaei, M.; Timmers, H.A.; Suarez-Diez, M.; Stams, B.S.G.H.v.J.M.; Plugge, M.C. Comparative proteomics of *Geobacter sulfurreducens* PCAT in response to acetate, formate and/or hydrogen in response to acetate, formate and/or hydrogen as electron donor. *Environ. Microbiol.* **2021**, *23*, 299–315. [[CrossRef](#)]

Disclaimer/Publisher's Note: The statements, opinions and data contained in all publications are solely those of the individual author(s) and contributor(s) and not of MDPI and/or the editor(s). MDPI and/or the editor(s) disclaim responsibility for any injury to people or property resulting from any ideas, methods, instructions or products referred to in the content.